ERDC Letter Report

Environmental Laboratory

US Army Corps of Engineers®
Engineer Research and Development Center

Modeling Sediment Transport in Grand Traverse Bay, Michigan to Determine Effectiveness of Proposed Revetment at Reducing Transport of Stamp Sands onto Buffalo Reef

August 2015

Earl Hayter, Ray Chapman, Lihwa Lin, Phu Luong, Greg Mausolf, Dave Perkey, Dave Mark, and Joe Gailani

Environmental and Coastal and Hydraulics Laboratories
U.S. Army Engineer Research and Development Center
3909 Halls Ferry Road
Vicksburg, MS 39180

Letter Report

The US Army Engineer Research and Development Center (ERDC) solves the nation's toughest engineering and environmental challenges. ERDC develops innovative solutions in civil and military engineering, geospatial sciences, water resources, and environmental sciences for the Army, the Department of Defense, civilian agencies, and our nation's public good. Find out more at www.erdc.usace.army.mil.

To search for other technical reports published by ERDC, visit the ERDC online library at http://acwc.sdp.sirsi.net/client/default.

Modeling Sediment Transport in Grand Traverse Bay, Michigan to Determine Effectiveness of Proposed Revetment at Reducing Transport of Stamp Sands onto Buffalo Reef

Earl Hayter

Environmental Laboratory
U.S. Army Engineer Research and Development Center
3909 Halls Ferry Road
Vicksburg, MS 39180-6199

Ray Chapman, Lihwa Lin, Phu Luong, Dave Perkey, Dave Mark, and Joe Gailani

Coastal and Hydraulics Laboratory
U.S. Army Engineer Research and Development Center
3909 Halls Ferry Road
Vicksburg, MS 39180-6199

Greg Mausolf

Hydraulics & Hydrology Office

U.S. Army Corps of Engineers, Detroit District
477 Michigan Avenue
Detroit, MI 48226

Letter Report

Prepared for **U.S. Army Engineer District, Detroit**
Detroit, MI 48226

Abstract

The USACE Detroit District (LRE), ERDC, Michigan Technological University, and other government agencies (*e.g.*, EPA, State of Michigan) have been involved in monitoring the spread of sediment from the Gay, MI Stamp Sand deposits over several decades. LRE requested that ERDC develop a numerical hydrodynamic and mixed sediment transport model of the area of Lake Superior on the east side of the Keweenaw Peninsula. The sediment transport model for the contaminated Gay Stamp Sand deposits was used to predict the future spread of the deposits (both longshore and offshore) as well as the impact of alternative management actions. The model simulated two alternatives: 1) a without-project alternative (which is the existing condition), and 2) one with-project condition that represented a 6,600 linear ft rubble mound revetment that would serve as a barrier between the Stamp Sands deposits and the shoreline and littoral zone in front of the revetment. The model simulations of both alternatives were used to develop a ten-year sediment budget that allowed the percentage of Buffalo Reef that was covered with at least one inch (2.54 cm) of Stamp Sands for both alternatives to be determined. The initial condition, as determined from analysis of field sampling, used for both simulations was that Buffalo Reef is currently approximately 25 percent covered by Stamp Sands.

For the without-project alternative, an estimated 60 percent of Buffalo Reef will be covered by at least one inch of Stamp Sands over the next 10 years. Even for the with-project alternative, *i.e.*, with the proposed rubble-mound revetment, Stamp Sands already in the littoral zone will continue to move downdrift towards Buffalo Reef and Grand Traverse Harbor. As a result, an estimated 35 percent of Buffalo Reef will be covered by at least one inch of Stamp Sands for the with-project alternative. This comparison of the model simulations of the with-project and without-project alternatives simulations showed that the proposed rubble mound revetment alternative would satisfy the intended purpose of minimizing the offshore transport of these contaminated sediments onto Buffalo Reef as well as their ongoing longshore transport.

Contents

Figures and Tables

Figures

Tables

1 Introduction

The USACE Detroit District (LRE), ERDC, and other government agencies (*e.g.*, EPA, State of Michigan) have been involved in monitoring the spread of sediment from the Gay Stamp Sand deposits over several decades. Figure 1-1 shows the Gay Stamp Sand deposits (inside the dashed red line) on the south shoreline of Michigan's Keweenaw Peninsula in Lake Superior as well as Buffalo Reef. The approximate extent of the longshore migration of these sands is seen in this figure to be to the Grand Traverse Harbor breakwall. Figure 1-2 shows a view of the northern end of the Stamp Sands deposits, while Figure 1-3 shows an oblique view of the Stamp Sand deposits. Figure 1-4 shows a photograph of the Stamp Sand deposits and the Lake Superior shoreline in front of the deposits.

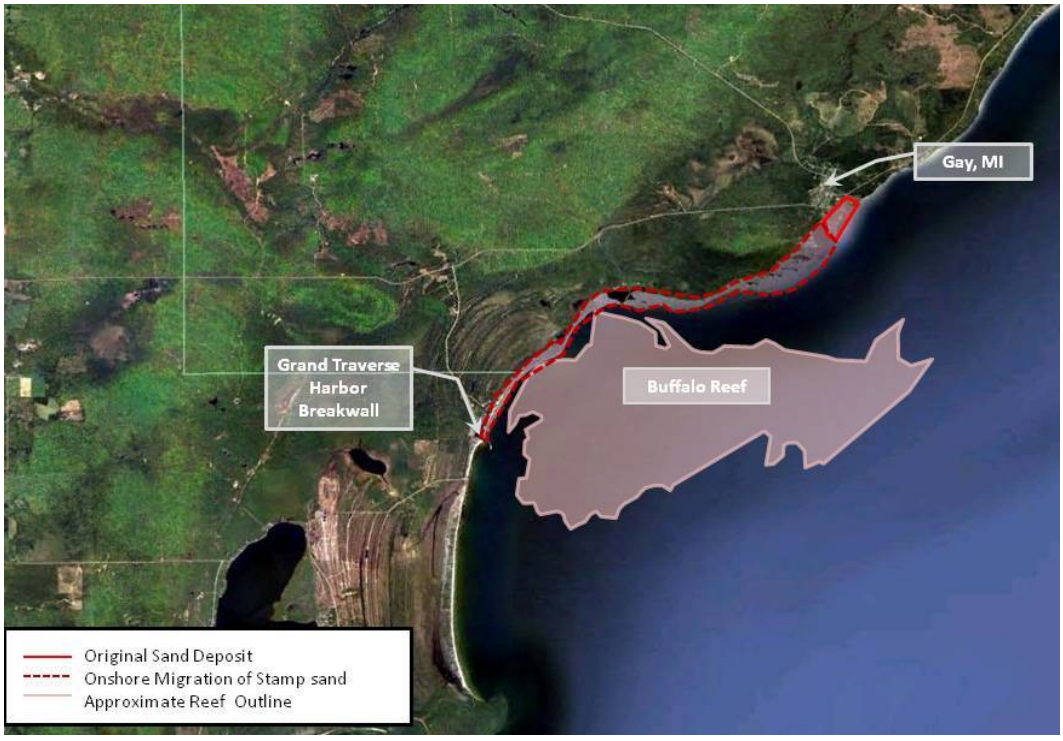

Figure 1-1 Gay Stamp Sand Deposits and Buffalo Reef

These legacy deposits are contaminated and are spreading offshore, including into both the trough (see Figure 1-5) and onto Buffalo Reef, as well as longshore. The contaminants sorbed to these sediments include metals (*e.g.*, copper, silver, and arsenic) which are all bioavailable.

Figure 1-2 Northern end of the Gay Stamp Sand Deposits

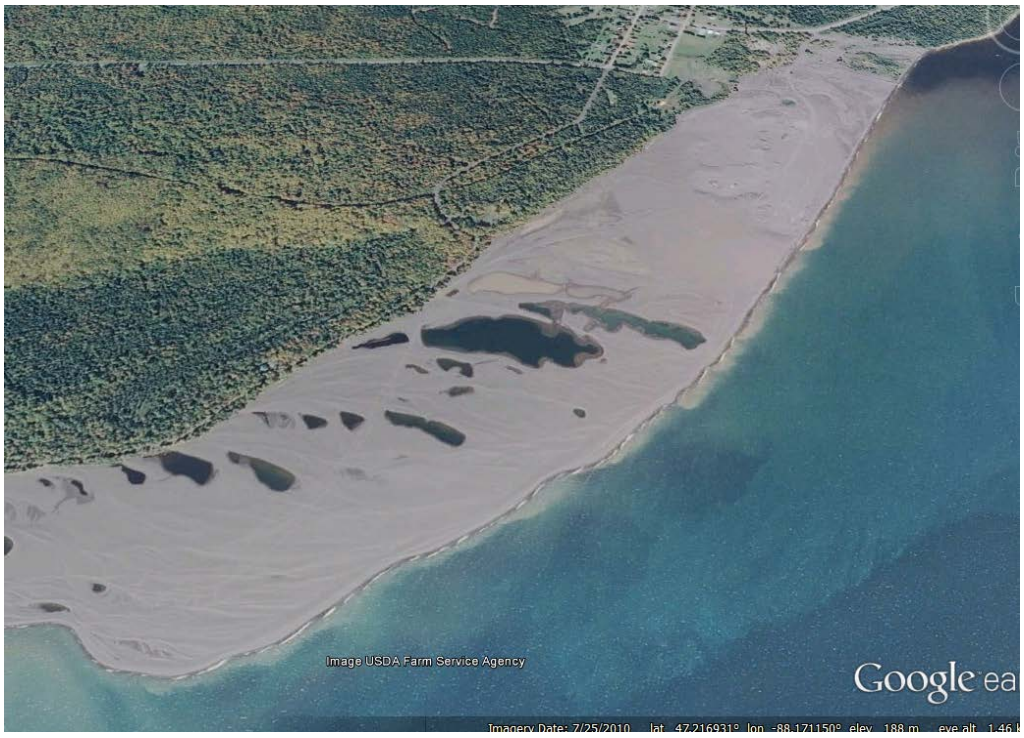

Figure 1-3 Oblique view of the Gay Stamp Sand Deposits

Figure 1-4 View to the south of Stamp Sand Deposits

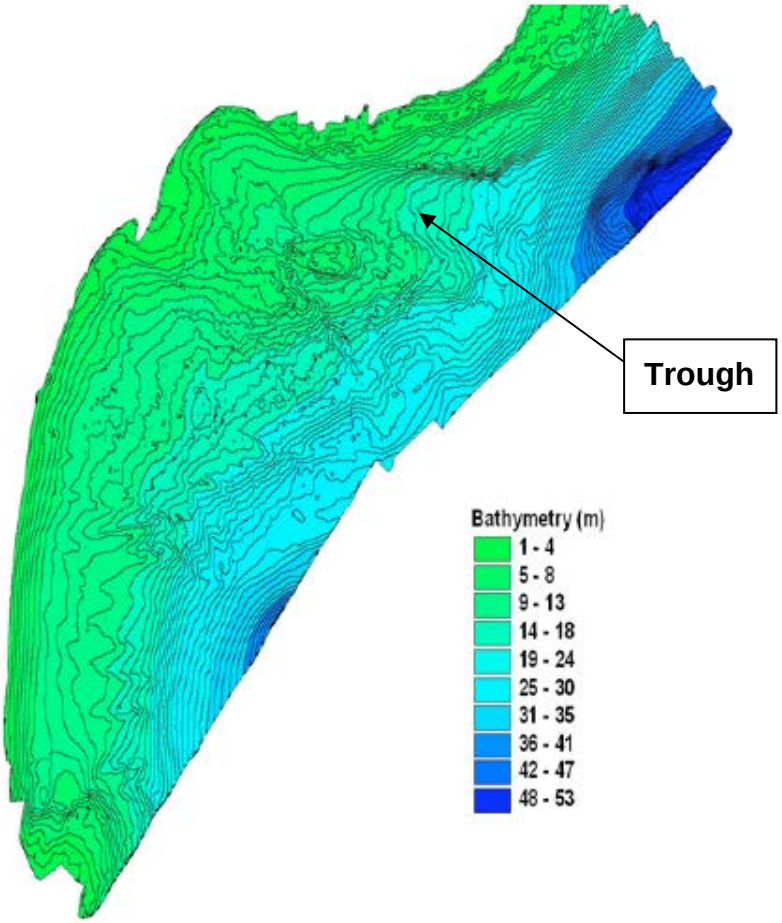

Figure 1-5 Bathymetry of Keweenaw Bay and the trough

Buffalo Reef is a productive spawning area for whitefish and lake trout that are potentially threatened by the transport of the Stamp Sands (Chiriboga and Mattes 2008). The movement of Stamp Sands into the cobble fields that surround Buffalo Reef is not conducive to hatching of fish eggs, for the sands may fill crevices or may be toxic for eggs or newly hatched larvae (Chiriboga and Mattes 2008).

The monitoring data that have been collected by State and Federal agencies and by Dr. Charles Kerfoot at the Michigan Technological University in Houghton, MI provide an understanding of how the sediments that have been eroded from the original pile are spreading in both the longshore and offshore directions. Studies using these data have revealed that the Stamp Sand deposits pile has been retreating at approximately 26 ft (7.9 m) per year for more than the past half century primarily due to erosion caused by wave and ice action at the base of the deposits well as fluctuating water levels in Lake Superior (Kerfoot 2___). This retreat of the Stamp Sands original pile has resulted in 67,000 yd^3 (CY) of contaminated Stamp Sands being added to the littoral zone in front of the original pile per year.

LRE has proposed to construct a 6,600 ft (2,012 m) rubble mound revetment in front of the original pile of Stamp Sand deposits. The purpose of this revetment is for source control, *i.e.*, it would eliminate the main source of the contamination by preventing an additional 67,000 yd^3 of Stamp Sands from being placed into Lake Superior each year. This remedial action would allow for initiation of restoration activities in proximity of Buffalo Reef and would also provide a protected placement site for dredged Stamp Sand material. Figure 1-5 shows the rubble mound revetment (that consists of both the red and blue lines) superimposed on the 2010 Stamp Sands shoreline. LRE requested that the U.S. Army Engineer Research and Development Center Environmental (ERDC-EL) and Coastal and Hydraulics (ERDC-CHL) laboratories develop a sediment transport model of the area of Lake Superior on the southern side of the Keweenaw Peninsula to evaluate the effectiveness of the proposed revetment in reducing the quantity of contaminated Stamp Sands that are being transported along the shoreline as well as offshore such as onto Buffalo Reef. This ERDC Letter Report describes the modeling study performed as well as the modeling results that were obtained.

Objectives

The objectives of ERDC's modeling study performed to accomplish the task requested by LRE were the following:

1. Develop a three-dimensional (3D) numerical hydrodynamic and sediment transport model that can be used to predict the future spread (in both the longshore and offshore directions) of Stamp Sand deposits along the Keweenaw Bay shoreline as well as the impact of alternative management actions. The model needed to have a flexible framework that could be modified to simulate multiple project conditions and also simulate other Stamp Sand sites on the shorelines of the Keweenaw Peninsula.

2. Use the model to simulate a without project condition (*i.e.*, no rubble mound revetment) and one with-project condition which is the 6,600 ft rubble mound revetment (see Figure 1-6).

3. Analyze the results to determine the effectiveness of the proposed revetment in reducing transport of Stamp Sands onto Buffalo Reef.

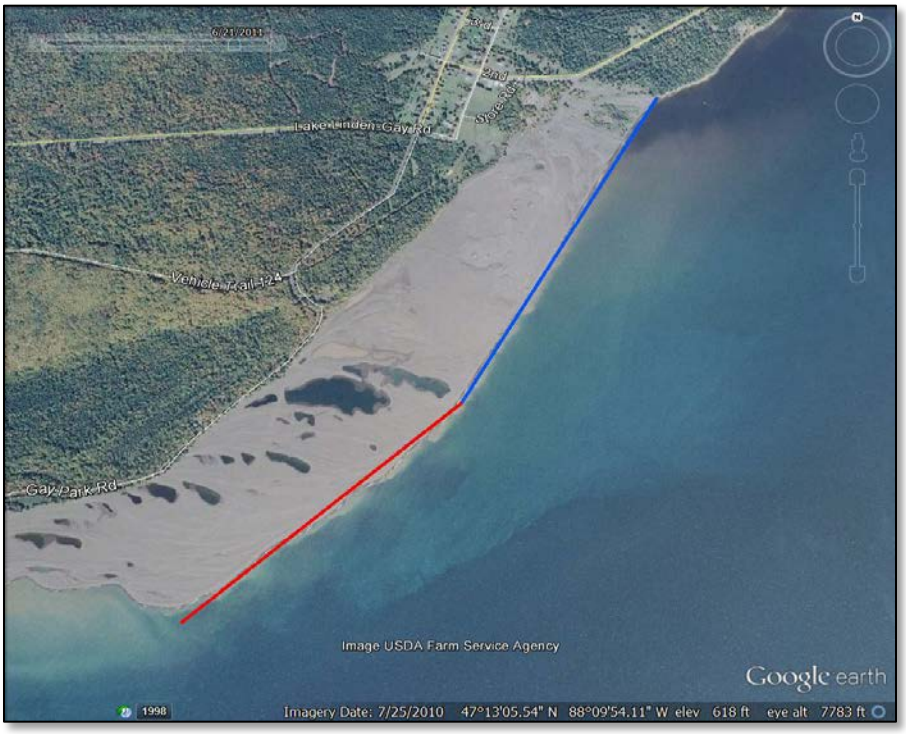

Figure 1-6 Rubble mound revetment (red and blue lines) superimposed on the 2010 Stamp Sands shoreline

Study Tasks

The following specific tasks were performed to accomplish the stated objectives.

Task 1. Hydrodynamic Modeling

Lake Superior hydrodynamics were simulated for the chosen time periods and specific storm events using the ADCIRC storm surge model for Lake Superior that was provided by the FEMA Modeling Contractor STARR (2012). A detailed description of ADCIRC is available at http://www.adcirc.org. The model's finite element mesh in Keweenaw Bay (see Figure 1-4) and in particular in Grand Traverse Bay that includes Buffalo Reef and the waters offshore of the Stamp Sands deposits and was refined to more accurately represent the highly variable bathymetry in the project area.

Figure 2-3 shows the mesh and model domain for the Lake Superior ADCIRC model. Predicted water surface elevation time series from the simulated time periods and storm events were used as the hydrodynamic boundary conditions for ERDC's Geophysical Scale Transport Modeling System (GSMB). GSMB is described in Section 2 along with its application to Lake Superior. GSMB contains the mixed sediment transport model (that is dynamically linked to the hydrodynamic model) that was used to simulate the transport of both Stamp Sands and native sediments. The hydrodynamic model in GSMB was used to simulate the 3D hydrodynamics for the selected time periods and storm events before the sediment transport modeling was performed to insure that no instabilities occurred.

Task 2. Wave Modeling

The CMS-Wave model, which is a spectral wave transformation model capable of simulating the formation, diffraction, refraction, reflection, and wave breaking of wind-generated surface waves, was used to model the selected time periods and storm events. This modeling is described in Section 3. Time series of wave properties (wave heights, periods and directions) were used in the mixed sediment transport model to calculate the spatially and temporally varying current- and wave-induced bed shear stresses. In addition, CMS-Wave predicted time series of radiation stress gradients that were used in the hydrodynamic model in GSMB to account for wave-induced effects on currents.

Task 3. Sediment Transport Modeling

The mixed sediment transport model in GSMB was setup using data analyzed from sediment samples collected at the Stamp Sands deposits pile as well as along the shoreline downdrift of the pile and at different locations in the trough and on Buffalo Reef. Next the sediment transport model was calibrated and partially validated using morphological changes obtained from LiDAR surveys of Grand Traverse Bay performed in 2008, 2010, 2011, and 2013 that quantifies the movement of Gay Stamp Sand deposits. Then GSMB was used to simulate the 3D hydrodynamics and sediment transport for the selected time periods and seven selected storm events for both the without and with project conditions. Ice-induced transport of Stamp Sands was not modeled. The sediment transport modeling performed is described in Section 4.

Task 4. Analysis of Modeling Results

The results were analyzed to determine 10-year predictions of sediment transport and the resulting morphological changes for both the without and with project conditions. Percentages of Buffalo Reef that would be covered with at least one inch (2.54 cm) of Stamp Sands for both cases were determined.

Report Layout

Chapter 2 describes the hydrodynamic modeling performed, Chapter 3 describes the wave modeling, and Chapter 4 describes the sediment transport modeling that was performed. Chapter 5 presents the results from the sediment transport modeling, and Chapter 6 presents the conclusions and recommendations from this modeling study.

2 Hydrodynamic Modeling

Modeling System

ERDC-EL and ERDC-CHL have completed a number of large scale hydrodynamic, sediment and water quality transport modeling studies. These studies have been successfully executed utilizing the Geophysical Scale Transport Modeling System (GSMB). The model framework of GSMB is shown in Figure 2-1, where it is seen that USACE accepted wave, hydrodynamic, sediment and water quality transport models are both directly and indirectly linked.

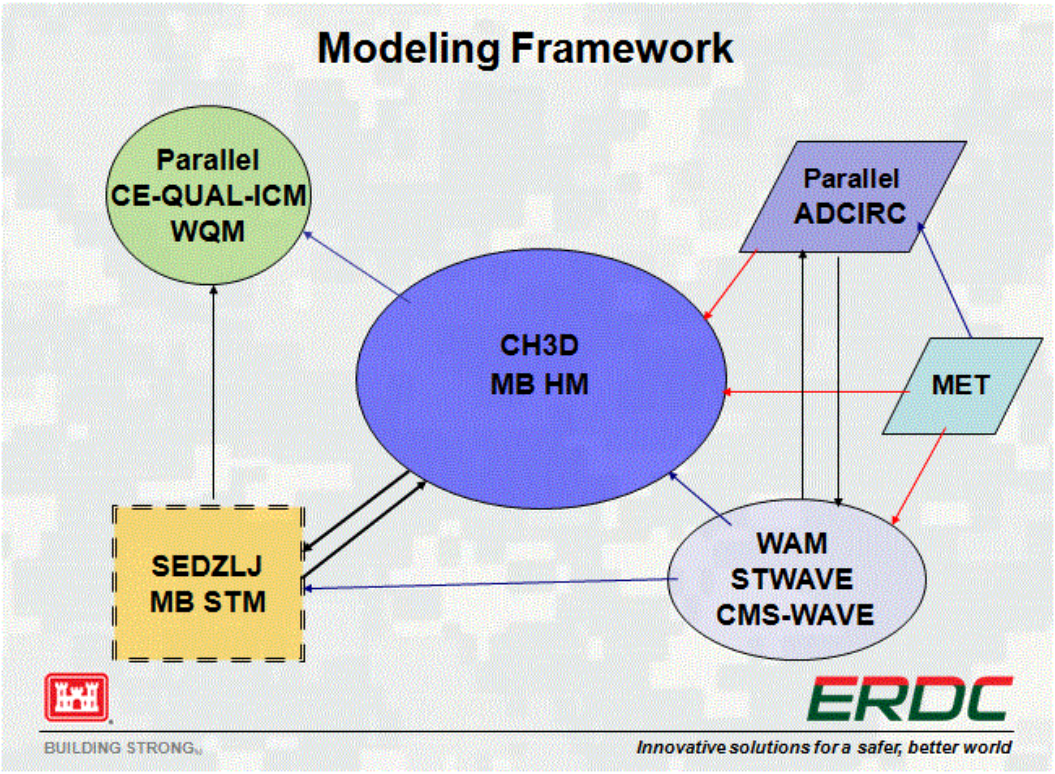

Figure 2-1 Multi-Block Geophysical Scale Transport (GSMB) Modeling System

The components of GSMB are the 2D deep water wave model WAM (Komen *et al.* 1994, and Jensen *et al.* 2012), shallow water wave models STWAVE (Smith *et al.* 1999) and CMS-WAVE (Lin *et al.* 2008), the large

scale unstructured 2D ADCIRC hydrodynamic model (http://www.adcirc.org) and the regional scale models CH3D-MB (Luong and Chapman 2009), which is the multi-block (MB) version of CH3D-WES (Chapman *et al*. 1996; Chapman *et al*. 2009), MB CH3D-SEDZLJ sediment transport model (Hayter *et al*. 2012), and CE-QUAL-ICM water quality model (Bunch *et al*. 2003, and Cerco and Cole 1994). For this study, a subset of GSMB components was applied where the meteorologically forced WAM provides the deep water wave forcing to CMS-WAVE, which in turn provides radiation stress gradients, wave heights, periods and directions forcing to MB CH3D-SEDZLJ. In addition, open water surface elevation forcing is provided to CH3D-SEDZLJ by the lake-wide ADCIRC simulations.

Meteorological Forcing: NCEP Climate Forecast System Reanalysis (CFSR) Wind and Pressure Fields

The NCEP Climate Forecast System Reanalysis (CFSR) archive is based on a re-analysis program of all meteorological products generated by NOAA's National Center for Environmental Predictions (http://rda.ucar.edu/pub/cfsr.html). This 33-year archive (1979 to 2011) provides wind and pressure on a Gaussian grid with resolution of approximately 38 km, and barometric pressure fields on a 0.5 deg global geographical resolution at one-hour intervals. The Lake Superior wind and pressure fields were downloaded, interpolated from the Gaussian grid to a spherical grid with a resolution of 0.02 deg in both longitude and latitude and reformatted by Oceanweather Inc. under contract to LRE for a 2012 FEMA project.

Refined ADCIRC Grid Simulations

The existing ADCIRC storm surge model bathymetry and grid, which were provided by the FEMA Modeling Contractor STARR (2012), are shown in Figures 2-2 and 2-3.

Additional grid improvement and refinement were implemented throughout Grand Traverse Bay and the Gay Stamp Sands site. Extensive calibration and validation storm event simulations were originally

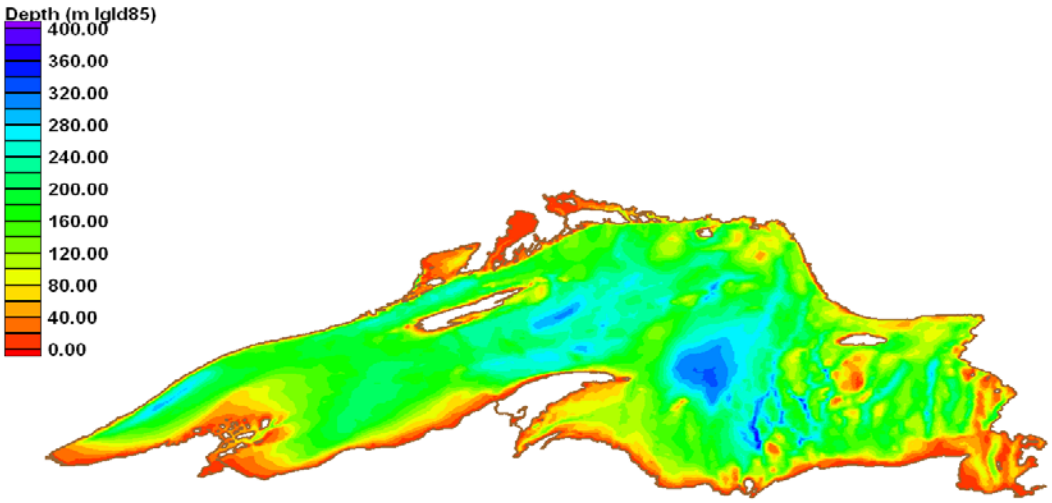

Figure 2-2 Lake Superior IGLD85 Bathymetry

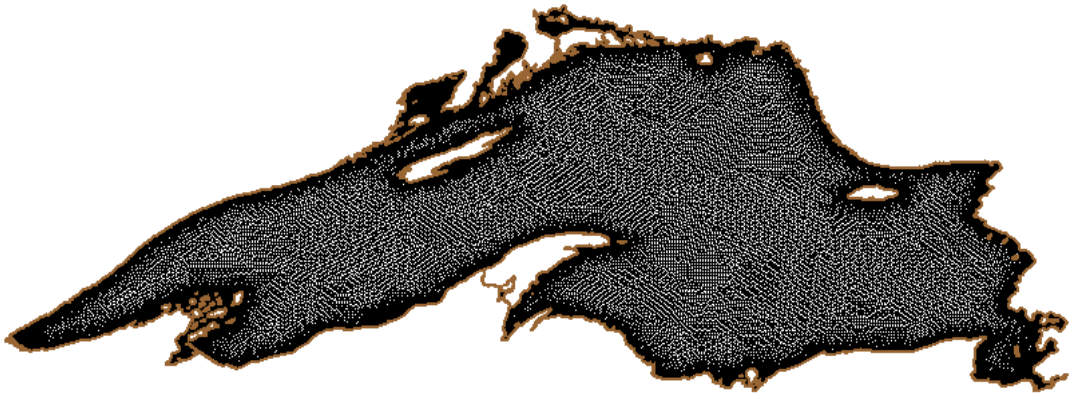

Figure 2-3 Lake Superior ADCIRC Grid

performed and analyzed by STARR (2012); however, the November 1994 1998 and April 2008 storm event simulations were selected to ensure the integrity of the updated refined grid via model data comparisons at Duluth and Pt. Iroquois. Given that Duluth, to the West, and Pt. Iroquois, to the East, are at opposite ends of Lake Superior, the water level response should be close to out of phase. Figures 2-4 and 2-5 show comparisons of model and observed water level variation during the November 1994 event in which good agreement is seen in both the magnitude and timing of water level set up and set down at both locations.

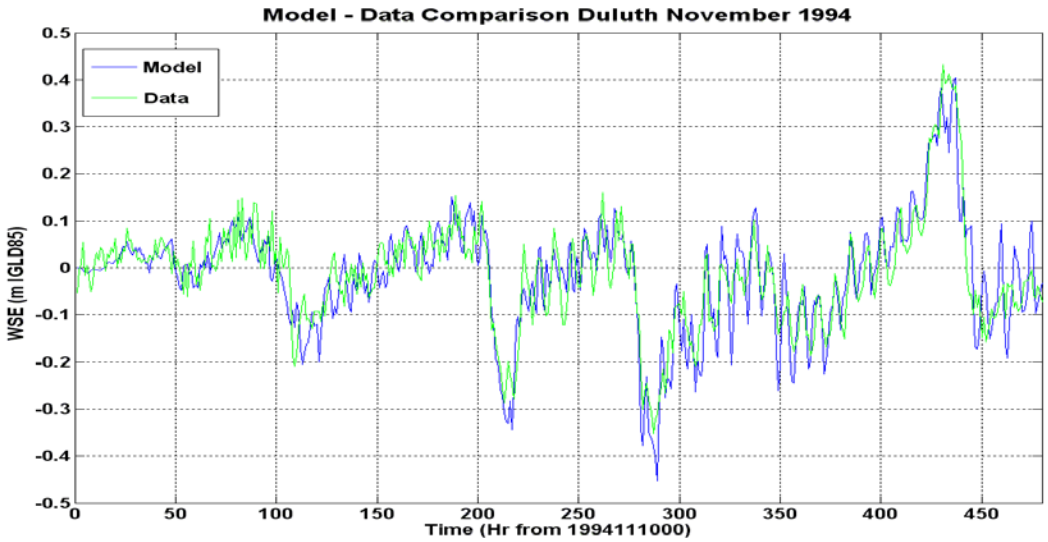

Figure 2-4 Duluth November 1994 Event Validation

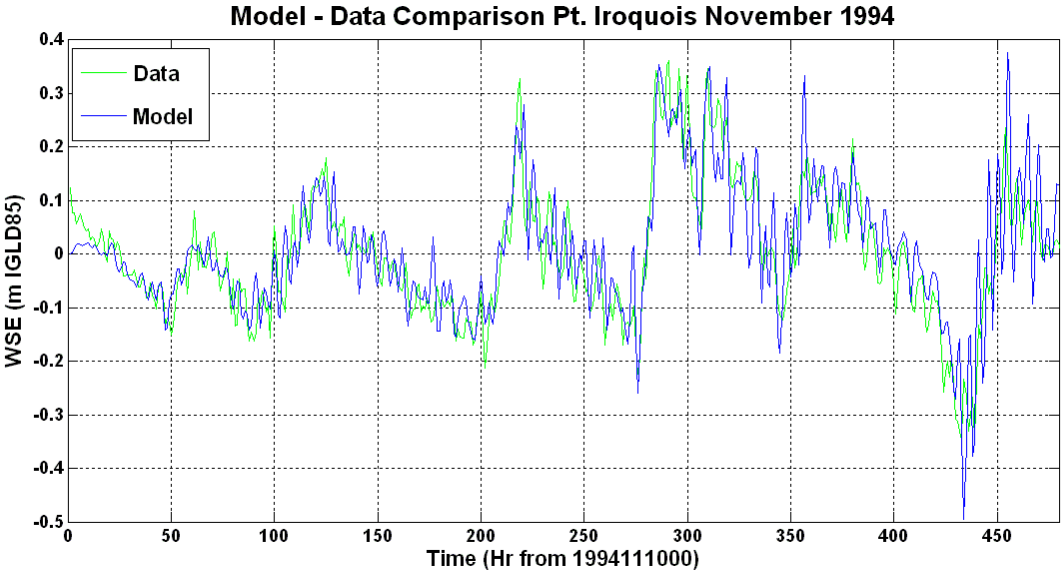

Figure 2-5 Pt. Iroquois November 1994 Event Validation

Similar results are seen for the November 1998 and April 2004 events in Figures 2-6 through 2-9.

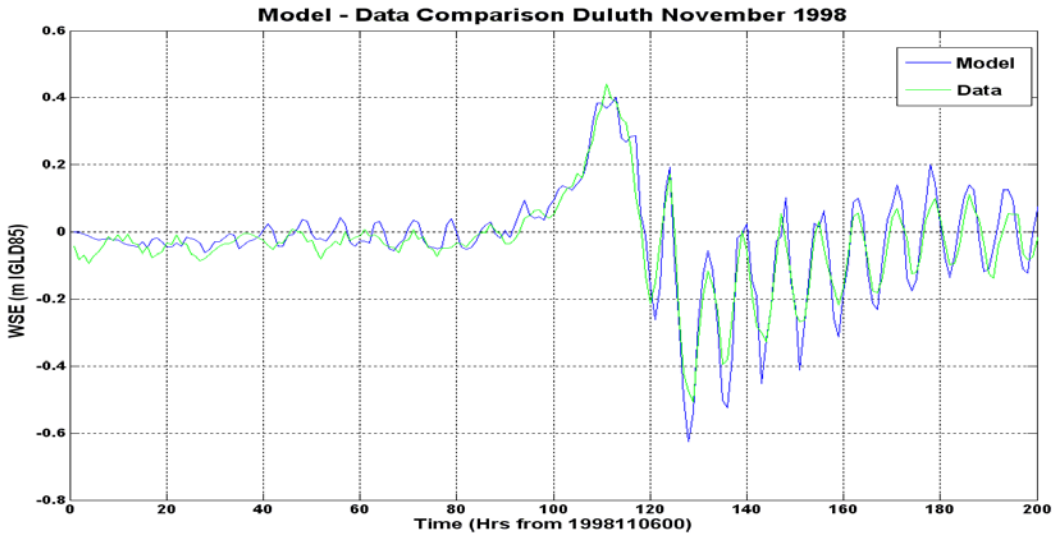

Figure 2-6 Duluth November 1998 Event Validation

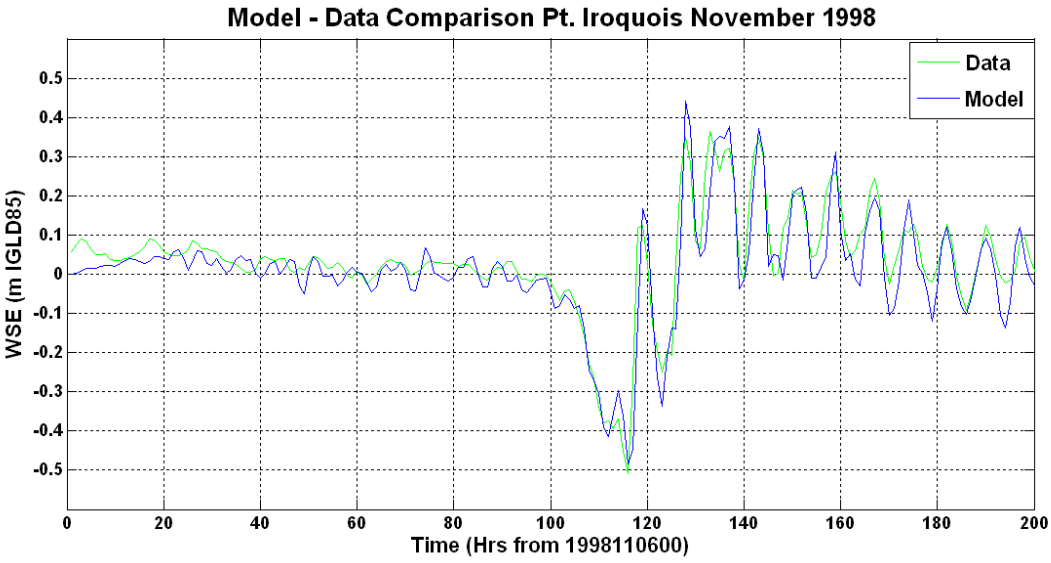

Figure 2-7 Pt. Iroquois November 1998 Event Validation

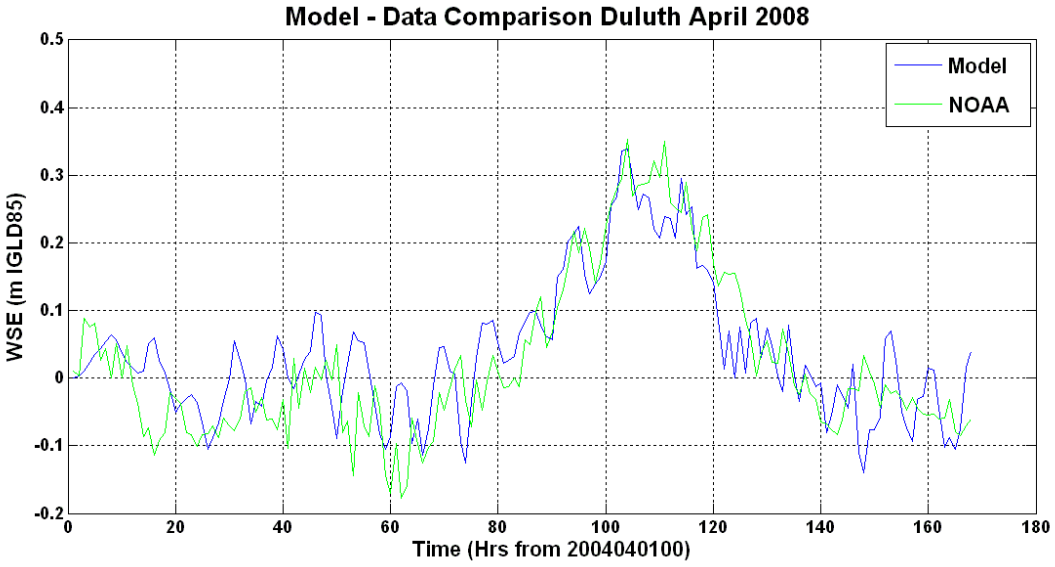

Figure 2-8 Duluth April 2008 Event Validation

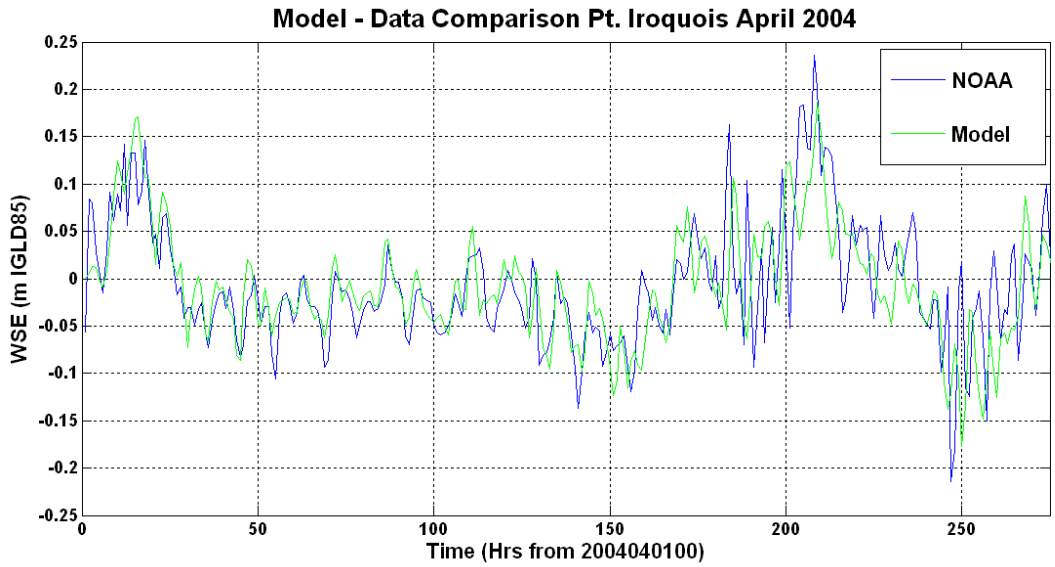

Figure 2-9 Pt. Iroquois April 2008 Event Validation

Having established the integrity of the updated ADCIRC model, open water surface elevation forcings for CH3D-SEDZLJ were developed for the non-storm and storm events and time periods shown in Tables 2-1 and 2-2, respectively. The simulations of sediment transport during both the non-storm and storm events shown in these two tables are described in

Section 4. Boundary forcings for the April - August and September - November time periods shown in Table 2-1 were generated with ADCIRC initialized to the still water level. In other words, the seasonal variation in lake level (Figure 2-10) is not represented in the simulations. To account for the seasonal variation in the boundary forcing, the observed water level data was time averaged to develop a set of linear segments that were added to the boundary input.

Table 2-1. Simulated Non-Storm Events

Case	Year	Duration
1a	2008	1 Apr – 31 Aug
1b	2008	1 Sep – 30 Nov
2a	2009	1 Apr – 31 Aug
2b	2009	1 Sep – 30 Nov
3a	2010	1 Apr – 31 Aug
3b	2010	1 Sep – 30 Nov
4a	2011	1 Apr – 31 Aug
4b	2011	1 Sep – 30 Nov
5a	2012	1 Apr – 31 Aug
5b	2012	1 Sep – 30 Nov
6a	2013	1 Apr – 31 Aug
6b	2013	1 Sep – 30 Nov

Table 2-2. Simulated Storm Events

Storm	Year	Duration
1	2007	21 Feb – 6 Mar
2	1985	11 Nov – 6 Dec
3	1990	9 – 30 Oct
4	1992	27 Oct – 17 Nov
5	1994	10 – 30 Nov
6	1995	11 – 28 Oct
7	1998	6 – 15 Nov

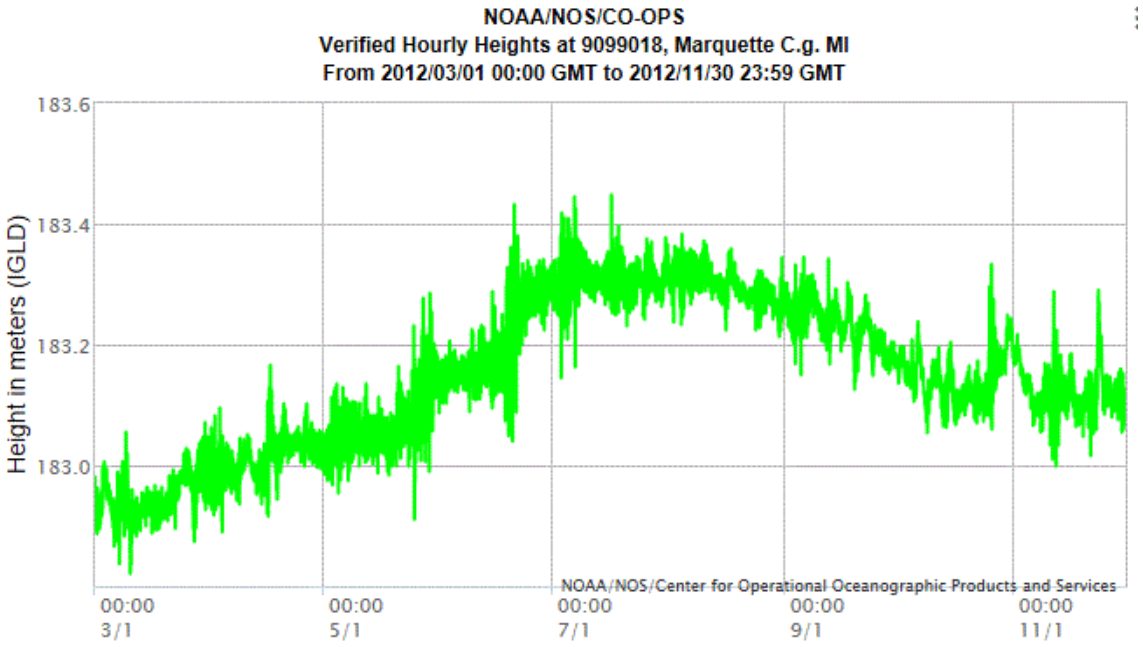

Figure 2-10 Seasonal Water Levels Observed at Marquette, 2012

Multi-Block Hydrodynamic Model Simulations

Hydrodynamic modeling of the Gay, MI Stamp Sands Site was performed with the three-dimensional (3D) hydrodynamic module of GSMB, CH3D-MB. Previous single-block applications of combined hydrodynamic and sediment transport models required long computer processing time as well as large memory storage requirements. This is because in structured grids with complicated geometries, the number of active cells (water) is often much smaller than the number of inactive cells (land). Both of these issues are overcome by implementation of single-block grid decomposition and Message Passing Interface (MPI) subroutines, which provide the multi-block grid capability (Snir *et al.* 1998). The MB grid approach runs each grid in parallel computations, where each grid block is assigned to a separate CPU or processor. Message passing allows the exchange of computational field information, such as the water surface elevation, velocity component and constituent arrays, between adjacent grid blocks. The advantages of the MB grid parallel approach include 1) the flexibility of site specific horizontal and vertical grid resolution assigned to each grid block, 2) block specific application of the sediment transport, wave radiation stress gradient forcing and computational cell wetting/drying

model options and 3) reduced memory and computational time requirements allowing larger computational domains and longer simulation time periods. Recent applications of the GSMB modeling system have included Mississippi Sound, which is a micro-tidal environment (Chapman and Luong 2009), and Cook Inlet, AK, which is a hypertidal estuary (Hayter *et al.* 2013).

The multi-block grid developed for the present study covered the region of Lake Superior from the northeast tip of the Keweenaw Peninsula to the coastline near Big Bay Point Lighthouse (Figure 2-11). The design of the grid systems allows 1) a boundary forcing sufficiently remote to the Stamps Sands site, 2) increasing grid resolution as one approaches Grand Traverse Bay (Figure 2-12) and 3) high resolution in the project area (10 – 20 m) (Figure 2-13). The initial bathymetry utilized in grid development is based on 2008 survey data (Figure 1-4), in which the trough to the north and northwest of Buffalo Reef is indicated.

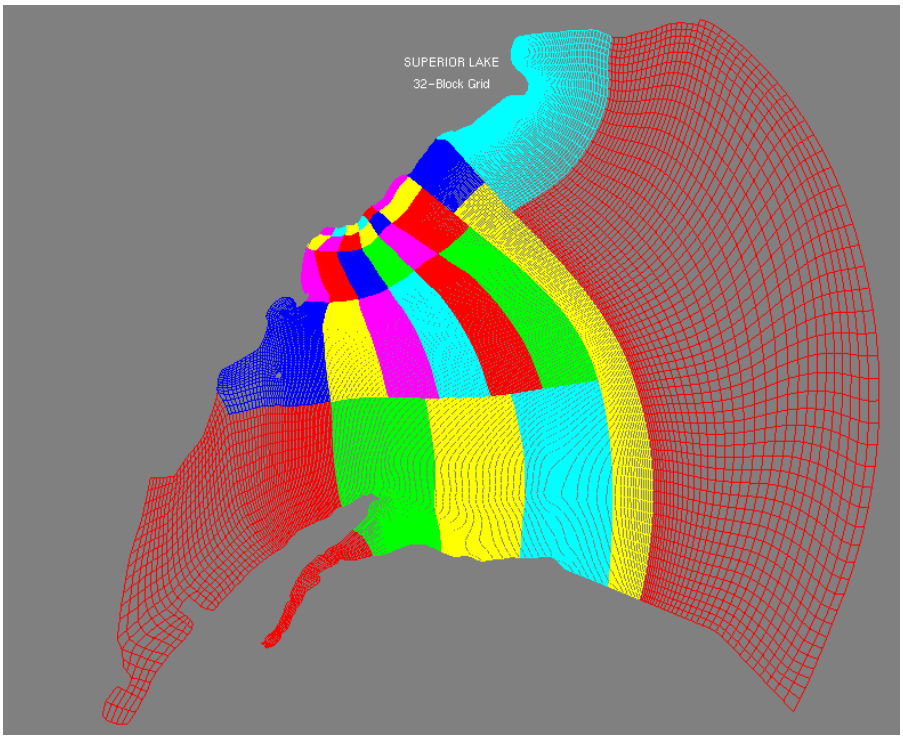

Figure 2-11 Stamp Sands 32 Block grid

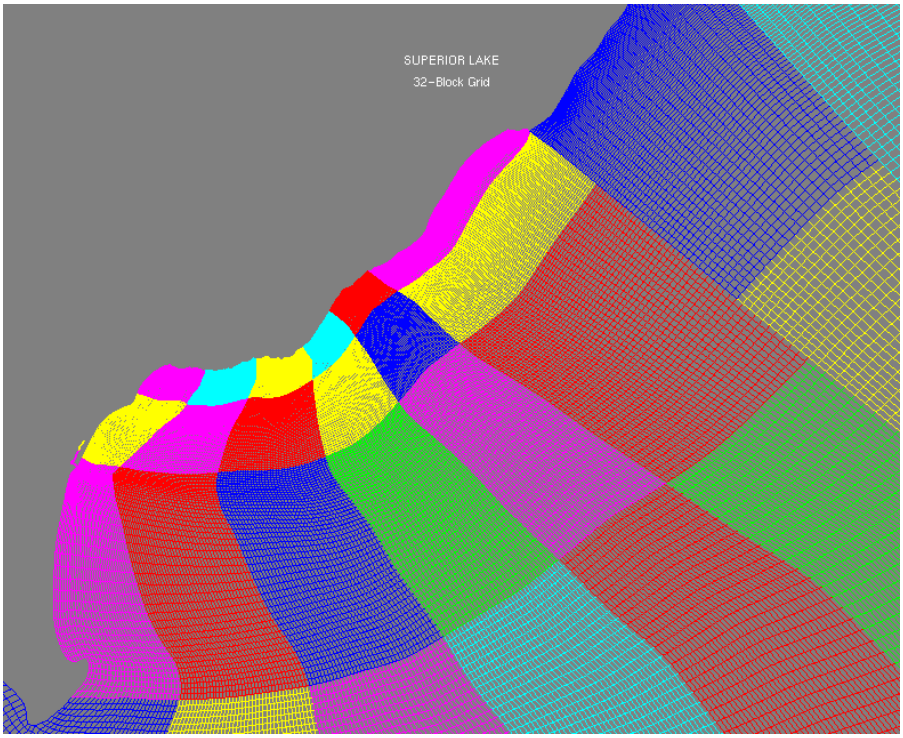

Figure 2-12 Mid-Resolution Region

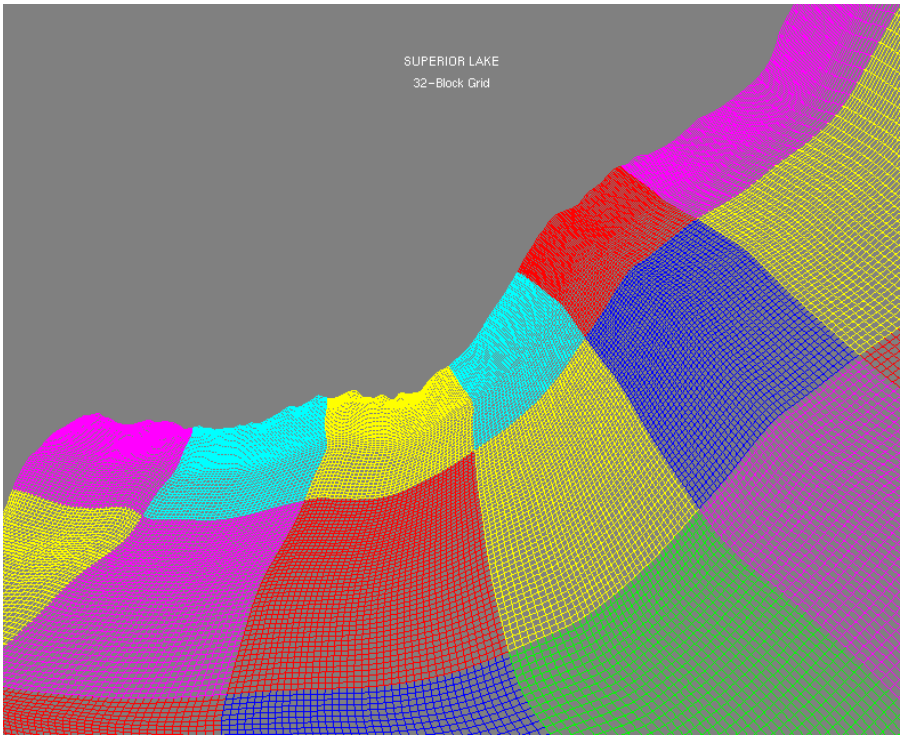

Figure 2-13 High-Resolution Site Blocks

3 Wave Modeling

Purpose

Wave heights, periods, directions and radiation stress gradients are required for the GSMB model simulations. Wave modeling was performed for the seven selected storms and the non-storm scenarios along the Grand Traverse Bay coastline. The WIS hindcast data from 1979 to 2012 (http://wis.usace.army.mil/hindcasts.shtml) were used to supply offshore boundary conditions for the wave modeling.

Wave Model

Wave modeling was conducted using CMS-Wave, a steady-state 2D spectral wave model (Lin *et al*. 2008; Lin *et al.* 2011a, 2011b) capable of simulating wave processes with ambient currents at coastal inlets and navigation channels. CMS-Wave is part of an integrated Coastal Modeling System (Demirbilek and Rosati 2011) developed at ERDC-CHL to assist in coastal region project applications.

CMS-Wave can be used either in half-plane or full-plane mode for wave transformation. It is based on the wave-action balance equation that includes wave propagation, refraction, shoaling, diffraction, reflection, breaking, and dissipation. The half-plane mode is default and CMS-Wave can run more efficiently in this mode as waves are transformed primarily from the seaward boundary toward shore.

In the present study, CMS-Wave was used to transform offshore wave information provided by WIS hindcast data to the Stamp Sands coast. The CMS-Wave uses the Surface-water Modeling System, SMS (Demirbilek *et al*. 2007; Zundel 2006) interface for grid generation, model setup, and post-processing.

Model Setup

Bathymetry Data

LRE provided available LiDAR data for Lake Superior that included the Stamp Sands coastline, Grand Traverse Bay, and Little Traverse Bay.

Model Grids

Figures 3-1 to 3-4 show the CMS-Wave modeling domain covering the Stamp Sands coastal region with the depth variation from four LiDAR surveys conducted in 2008, 2010, 2011, and 2013, respectively. The CMS model grid domain is approximately 3.7 mi x 9.3 mi (6 km x 15 km). The grid cell size varies from 30 ft to 330 ft (9 m to 100 m). The water depths in the model grid vary from 0 to 230 ft (0 to 70 m).

Forcing Conditions

The prevailing winds in Lake Superior generally blow across the lake from NW, N, NE, and sometimes from the E direction. Strong winds are a threat from fall through spring over the open lake waters. Winter winds remain strong, mostly out of the S through NW with an increase in northerlies. The Stamp Sands coastline is least susceptible to strong winds because it is rather sheltered to waves from W, NW and N.

Lake Superior is sufficiently large for strong winds from any direction to have long fetch to build up storms. Maximum waves in summer rarely reach 10 ft, and are 2 ft or less about 70 percent of the time, and large wave conditions generally occur during autumn. The Stamp Sands coastline is the least vulnerable while central and eastern water regions are more susceptible to the strong northerly and westerly winds.

During most winter months, the lake surface in different regions is 40 to 90 percent covered by ice, but rarely freezes over completely. Open water often persists in the lake center because the ice that forms there is blown or broken by strong winds. Over the past 30 years, the ice cover and duration have been diminishing as a result of regional warming, approximately $+1^0$ C/decade. The lake may briefly become covered 80 to 90 percent, but strong winds and large waves generally compact the thinner ice and stir up warm water, thus reducing the ice coverage to 40 to 50 percent during a severe winter season.

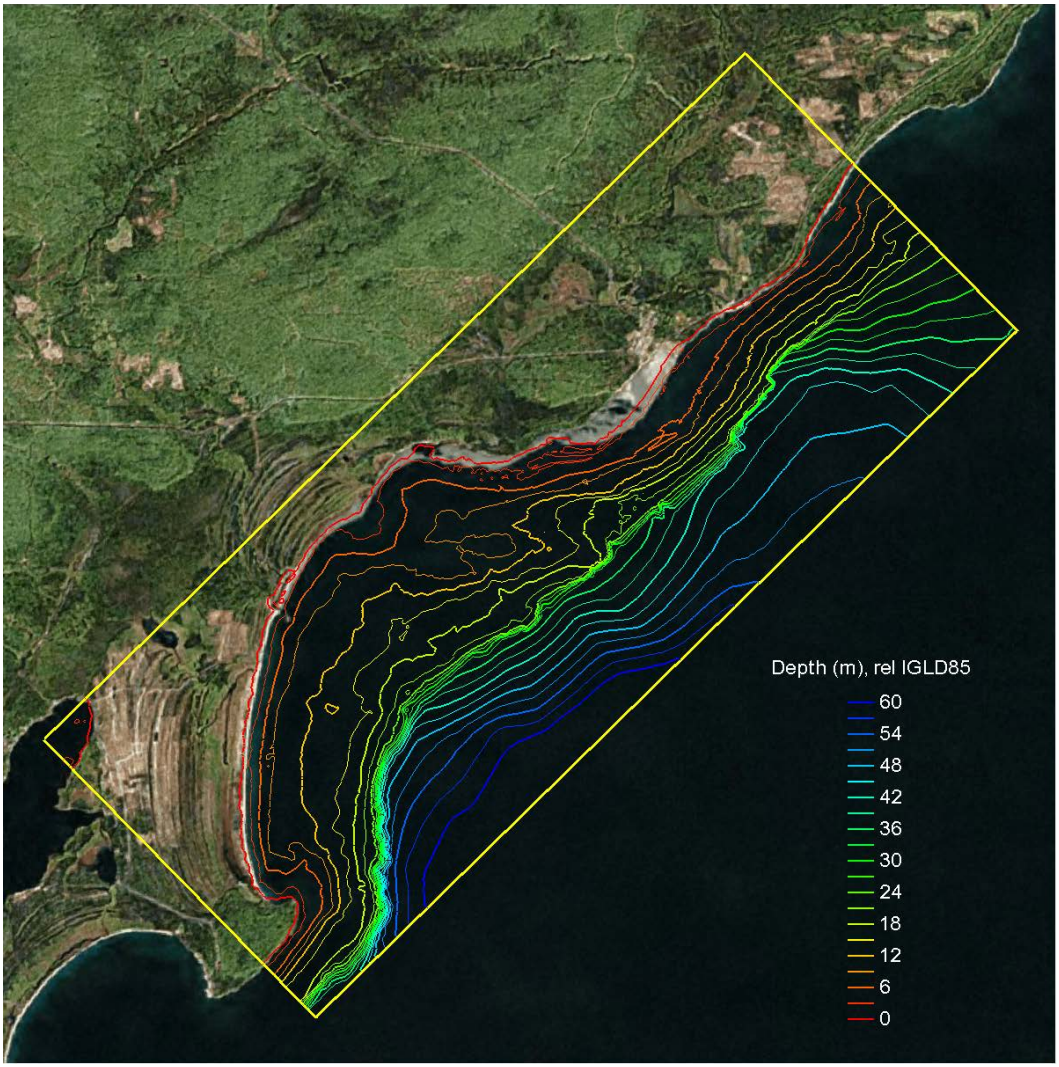

Figure 3-1. CMS-Wave model domain and depth contours based on 2008 LiDAR data.

The lake water level fluctuates, and normal elevation of the lake surface varies irregularly from year to year. The water surface is also subject to a consistent seasonal rise and fall. The lowest stage usually occurs in the late winter and the highest in the late summer. Strong lake winds and large barometric pressure changes that accompany squalls can produce fluctuations lasting at most a few hours up to a day. This fluctuation of water levels is called “lake seiching”, and seldom exceeds one foot (0.33 m) above or below the normal water daily level. The water level of Lake

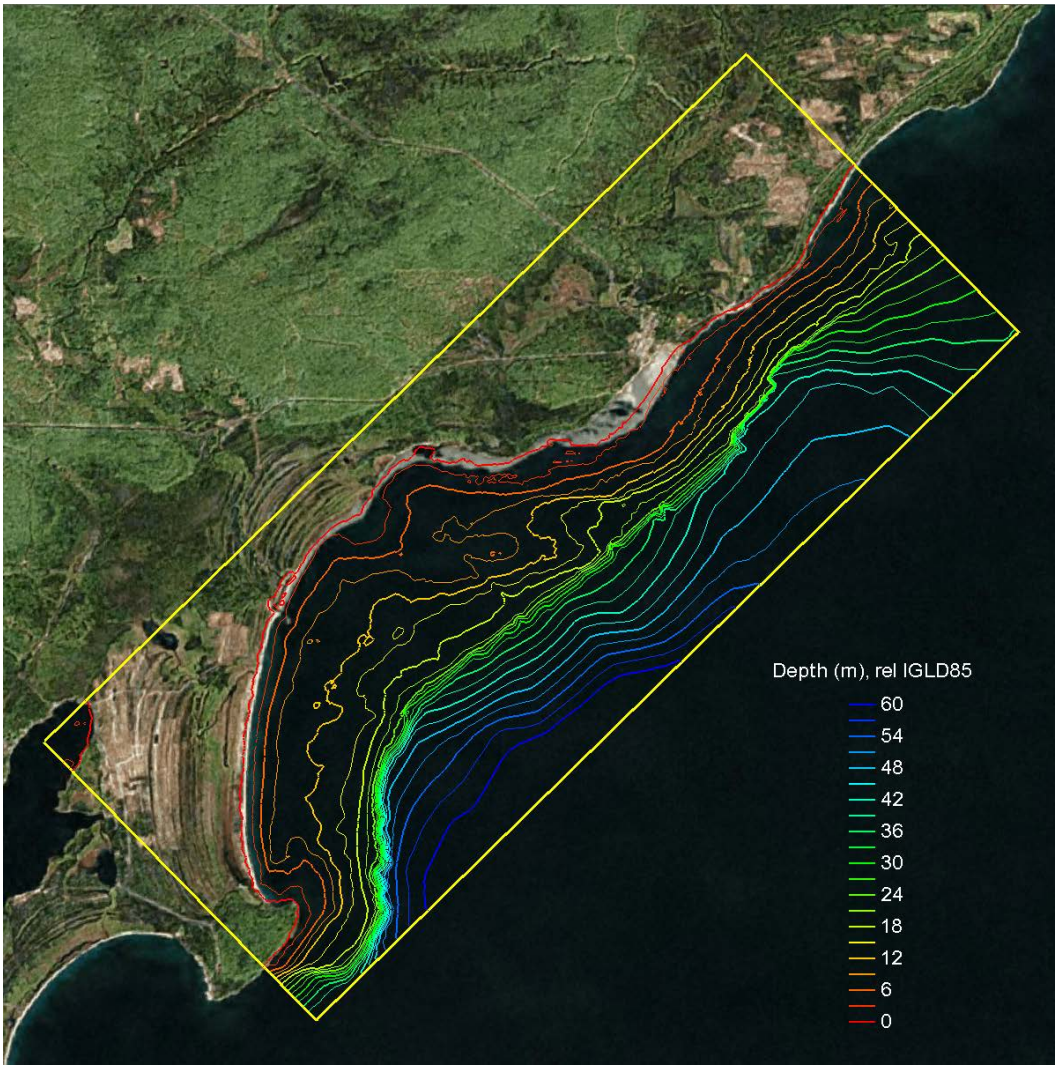

Figure 3-2. CMS-Wave model domain and depth contours based on 2010 LiDAR data.

Superior is partially controlled by means of dikes and sluice gates at the St Mary's River to maintain the monthly mean between elevations 599.61 ft (182.76 m) and 603.22 ft (183.86 m) on International Great Lakes Datum 1985 (IGLD85).

Water level measurements at the south lake region are available from two NOAA coastal stations (http://tidesandcurrents.noaa.gov/) shown in Figure 3-5. These are Marquette (Station 9099018) and Ontonagon (Station 9099044), MI. Figure 3-6 shows the water levels measured at these two stations for 2009-2012. The water level variations are generally

similar between the two stations with slightly more water level fluctuation at Marquette than at Ontonagon.

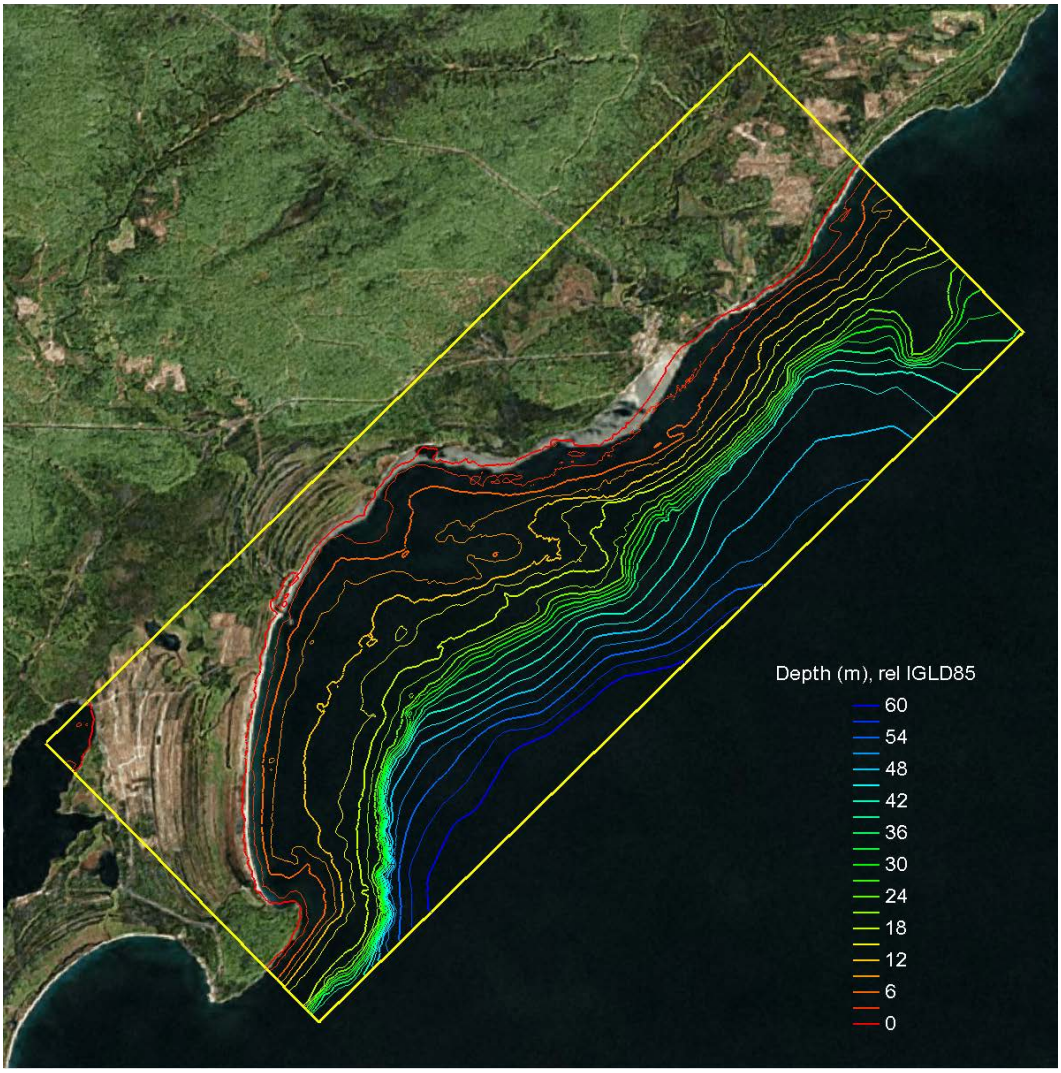

Figure 3-3. CMS-Wave model domain and depth contours based on 2011 LiDAR data.

Wind data for the south central Lake region are available from six NOAA stations at Grand Traverse Bay (GTRM4), Big Bay (BIGM4), Marquette (MCGM4), Stannard Rock (STDM4), Buoy 45004, and Buoy 45025 (Figure 3-7). Buoy 45025 is relative newer than other five stations as it was deployed in June 2011 while other Stations were installed prior to 2008. The Great Lakes buoys are normally deployed from late spring to late fall to avoid ice conditions. Wave data are available from Buoys 45004 and 45025 (directional).

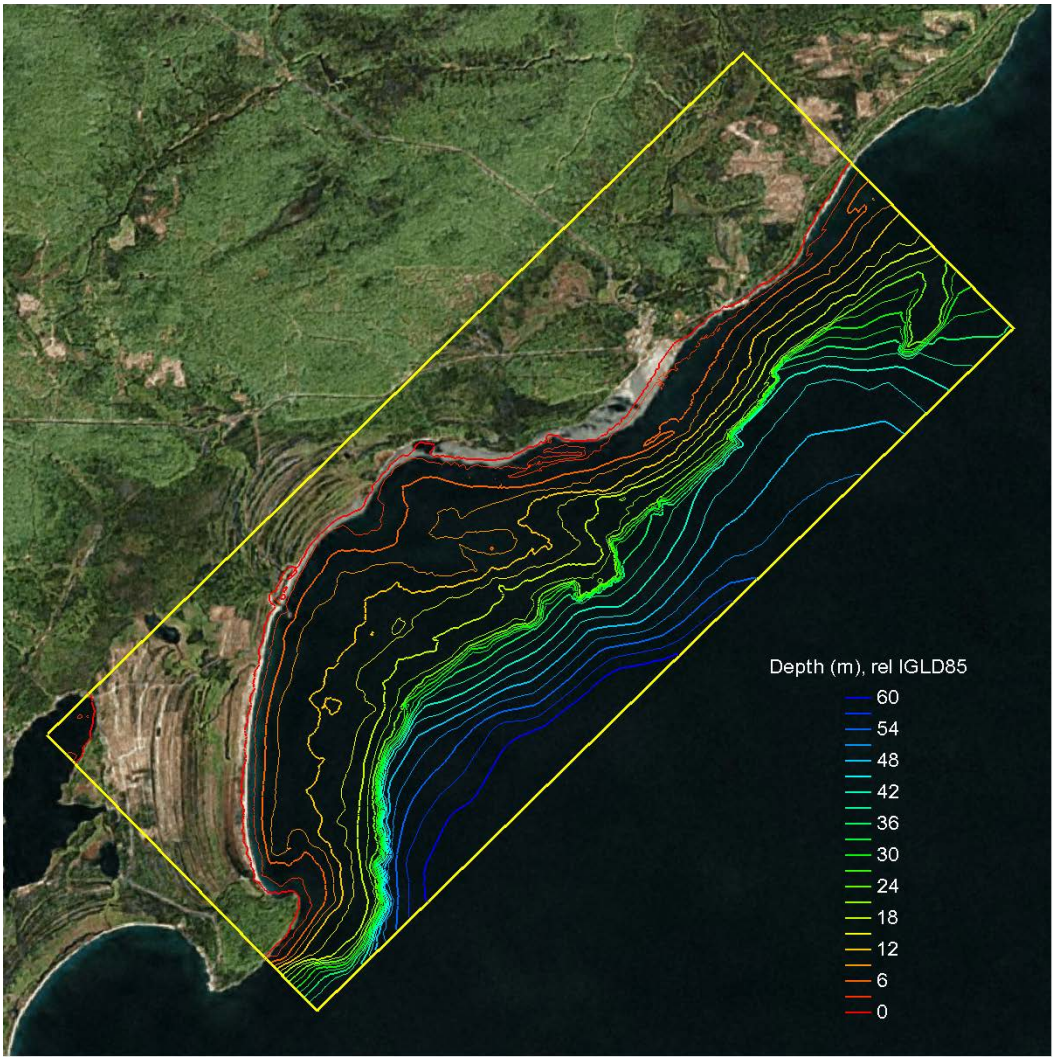

Figure 3-4. CMS-Wave model domain and depth contours based on 2013 LiDAR data.

Winds and waves affecting Stamp Sands and Grand Traverse Bay the most are those approaching from ENE, E, and ESE. Figures 3-8 and 3-9 show the 2012 sample wind data collected from BIGM4 and GTRM4, and from MCGM4 and STDM4, respectively. Figure 3-10 shows the wind and wave data from Buoys 45004 and 45025 for 2012. Overall comparison of the wind data shows wind speeds are greater at the open water stations (STDM4, 45004, and 45025) than at the coastal stations (BIGM4, GTRM4, and MCGM4). Wind directions at the coastal stations (BIGM4, GTRM4, and MCGM4) are also more influenced by the shoreline orientation owing to the land-water boundary effect.

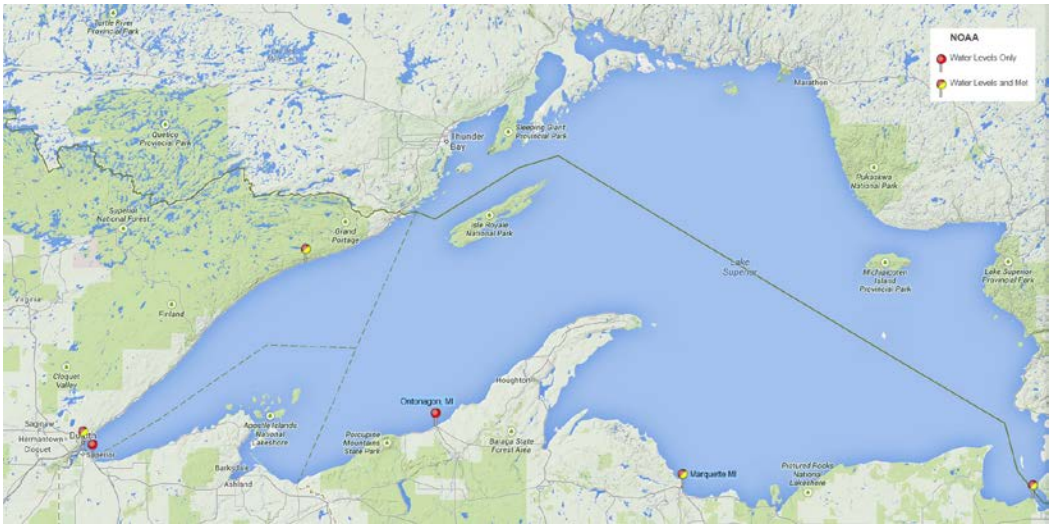

Figure 3-5. NOAA water level measurement stations in Lake Superior.

Additional wave information for Lake Superior is available from two databases: (1) 34 years hindcast database (1979-2012) from the Wave Information Study (WIS), and (2) approximately the last 8 year (2006-2014) nowcast data from the Great Lakes Coastal Forecasting System (GLCFS; http://www.glerl.noaa.gov/res/glcfs/). Figure 3-11 shows the available WIS Stations near Stamp Sands project site. Figure 3-12 shows a comparison of the GLCFS and WIS 2012 wind and wave data at WIS Sta 95113 (47.2 N, 88.12 W, depth = 55 m) offshore of the Stamp Sands site.

Comparison of GLCFS and WIS wave data at WIS Sta 95113 indicates the GLCFS nowcast wave heights and wave periods are generally greater than the WIS data while both databases provides similar wave directions. These nowcast and hindcast wave heights are less than 1 m about 90 percent of the year while larger waves (4 to 5 m height) can occur during storms. The peak wave period varies between 1 and 11 sec, and the majority of wave direction is from ENE and E sectors.

Figures 3-13 and 3-14 show the wind and wave roses, respectively, at WIS 95113 for the 34-year hindcast data (1979-2012). Figure 3-15 shows the corresponding extreme wave statistics analyzed for WIS 95113. The extreme waves approaching the Stamp Sands come more from the East direction with the maximum 34 year hindcast wave height equal to 4.7 m and wave period of 9.7 sec which corresponds to a 25 year return period.

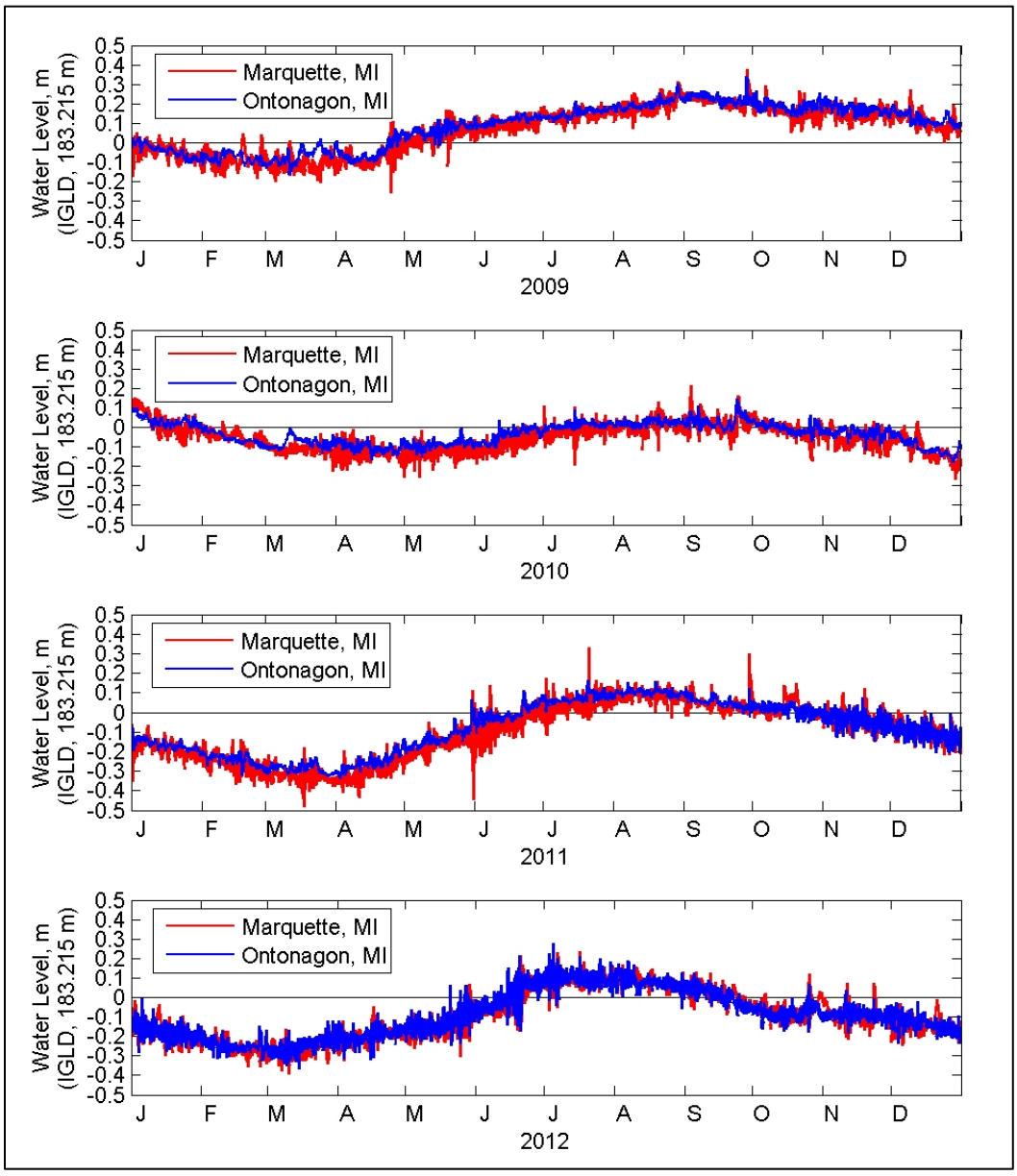

Figure 3-6. Water levels for 2009-2012 from NOAA stations at Marquette and Ontonagon, MI.

Figure 3-7. NOAA wind and wave measurement stations.

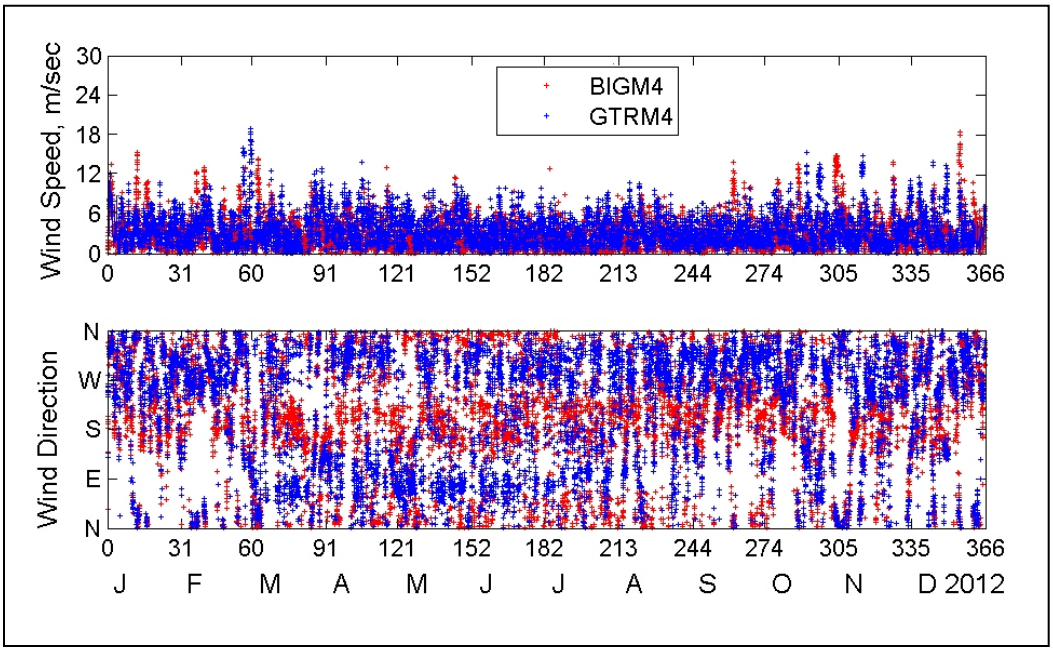

Figure 3-8. Wind measurements from BIGM4 and GTRM4 for 2012.

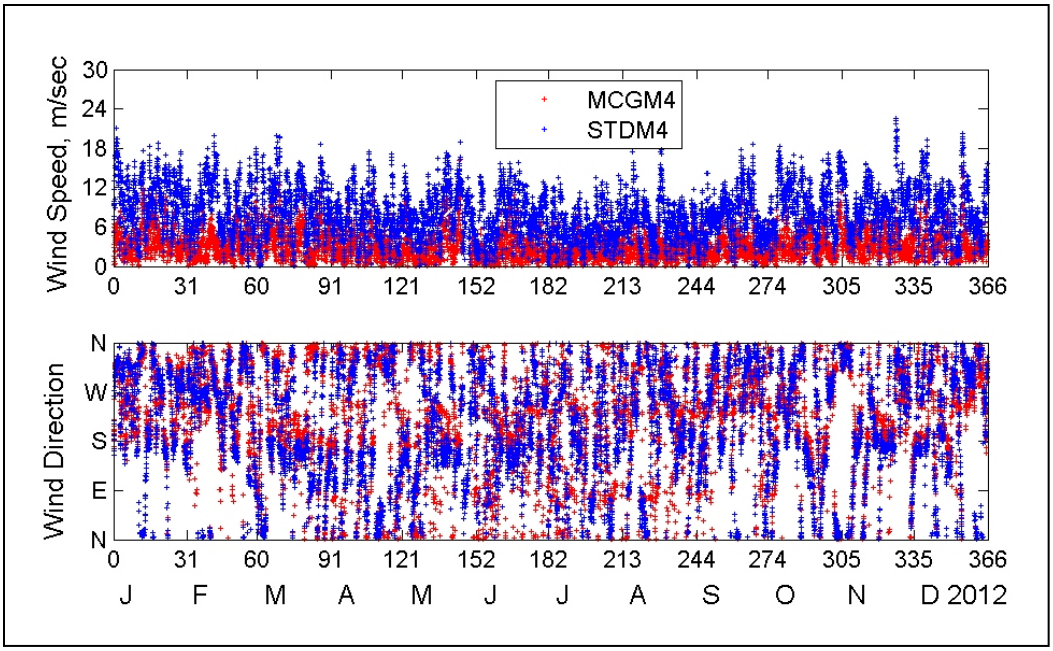

Figure 3-9. Wind measurements from MCGM4 and STDM4 for 2012.

Model Simulations

A total of 28 wave simulations were conducted, including 14 non-storm simulations and 14 storm simulations for both the existing site configuration and the one revetment design site configuration. Tables 3-1 and 3-2 listed the non-storm and storm wave cases, respectively. For the non-storm cases, two time periods of May-August (4 months) and October-November (2 months) were modeled in 3-hr interval for 2008, 2010, 2011, and 2013. For the storm cases, seven historical storms, with the duration from 10 days to 3 weeks, between 1985 and 2007 were selected and modeled in 1-hr interval.

The revetment configuration was simulated only for the CMS-Wave grid with the 2013 bathymetry survey (LiDAR) data. Figure 3-16 shows the depth contours with and without revetment configuration at the north side shoreline of Grand Traverse Bay. All 28 wave simulations include the water level variation data obtained from the NOAA coastal station at Marquette, MI. Because the wave model domain is relatively small compared to the much longer fetch in the lake, wind input was excluded in the simulations. Wave input was based on WIS data for all cases except 6a to 6d with the non-storm duration in 2013, not covered in the WIS

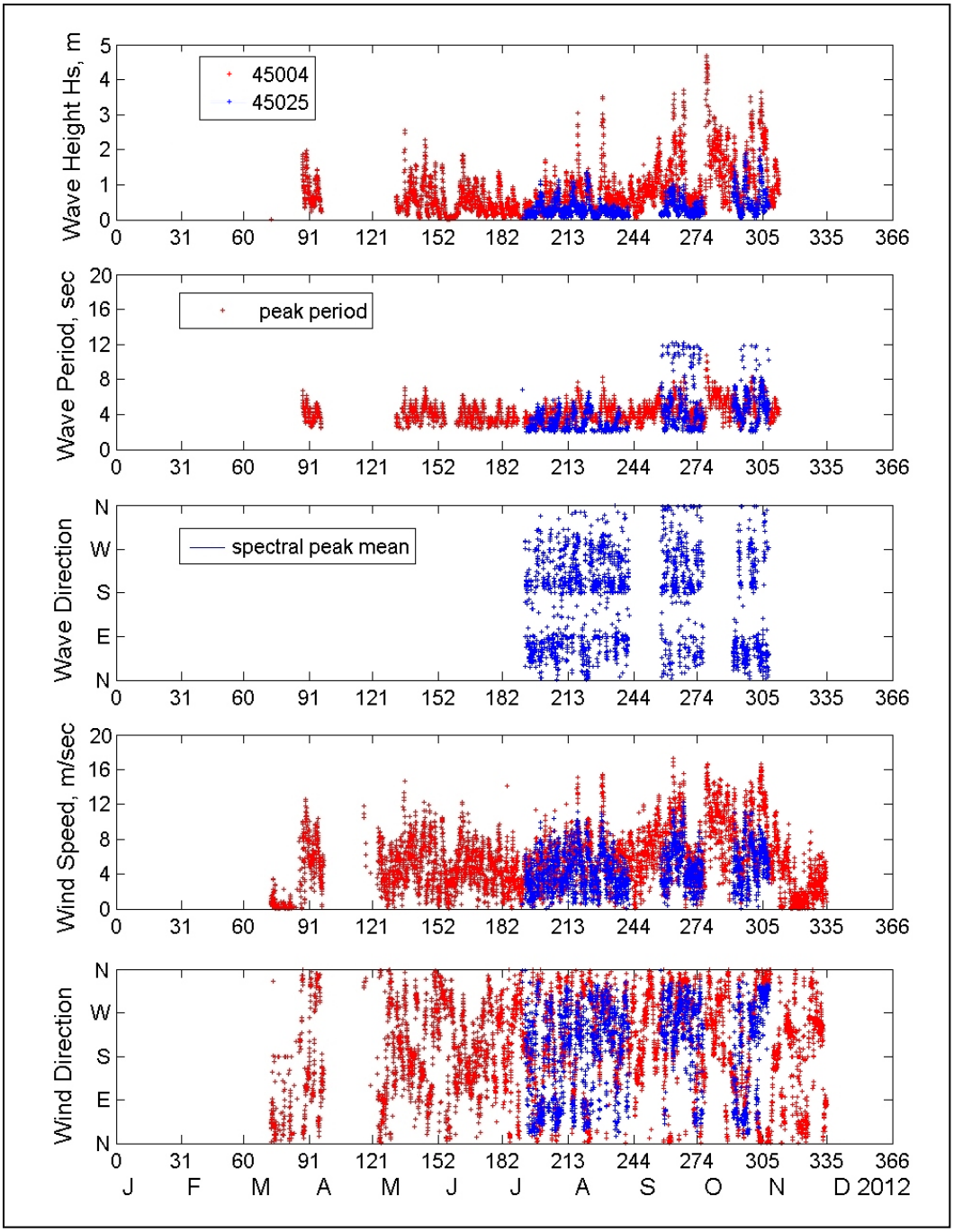

Figure 3-10. Wind and wave data from Buoys 45004 and 45025 for 2012.

database. Wave input for cases 6a to 6d was prepared based on GLCFS data. Figures 3-17 to 3-23 plot the time series of WIS data used for the offshore wave boundary conditions for seven simulated storms.

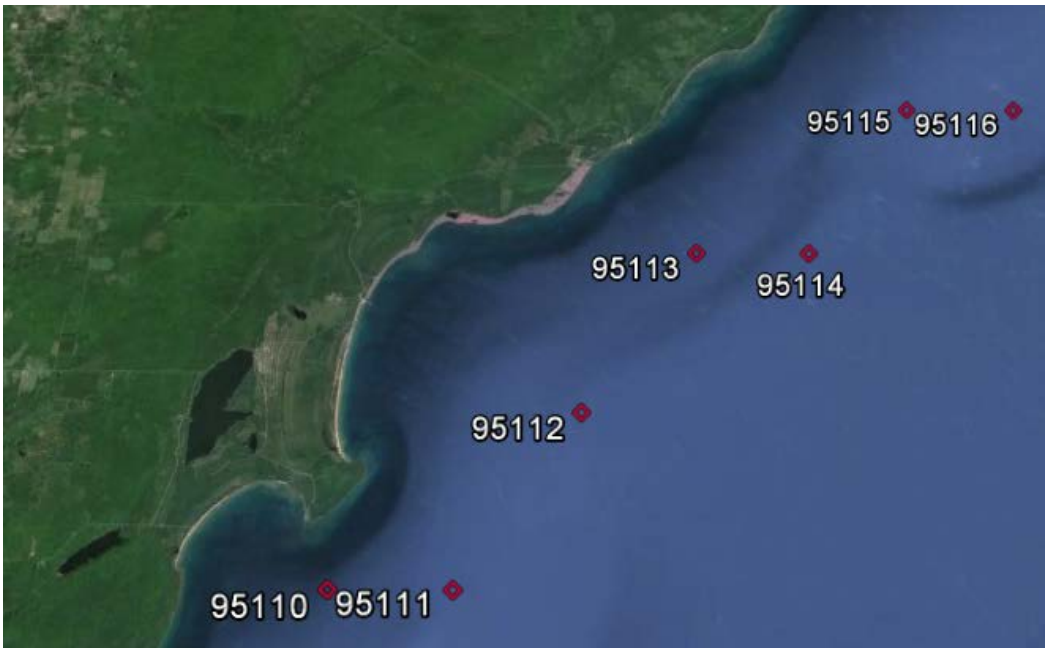

Figure 3-11. Location map for WIS stations near Stamp Sands.

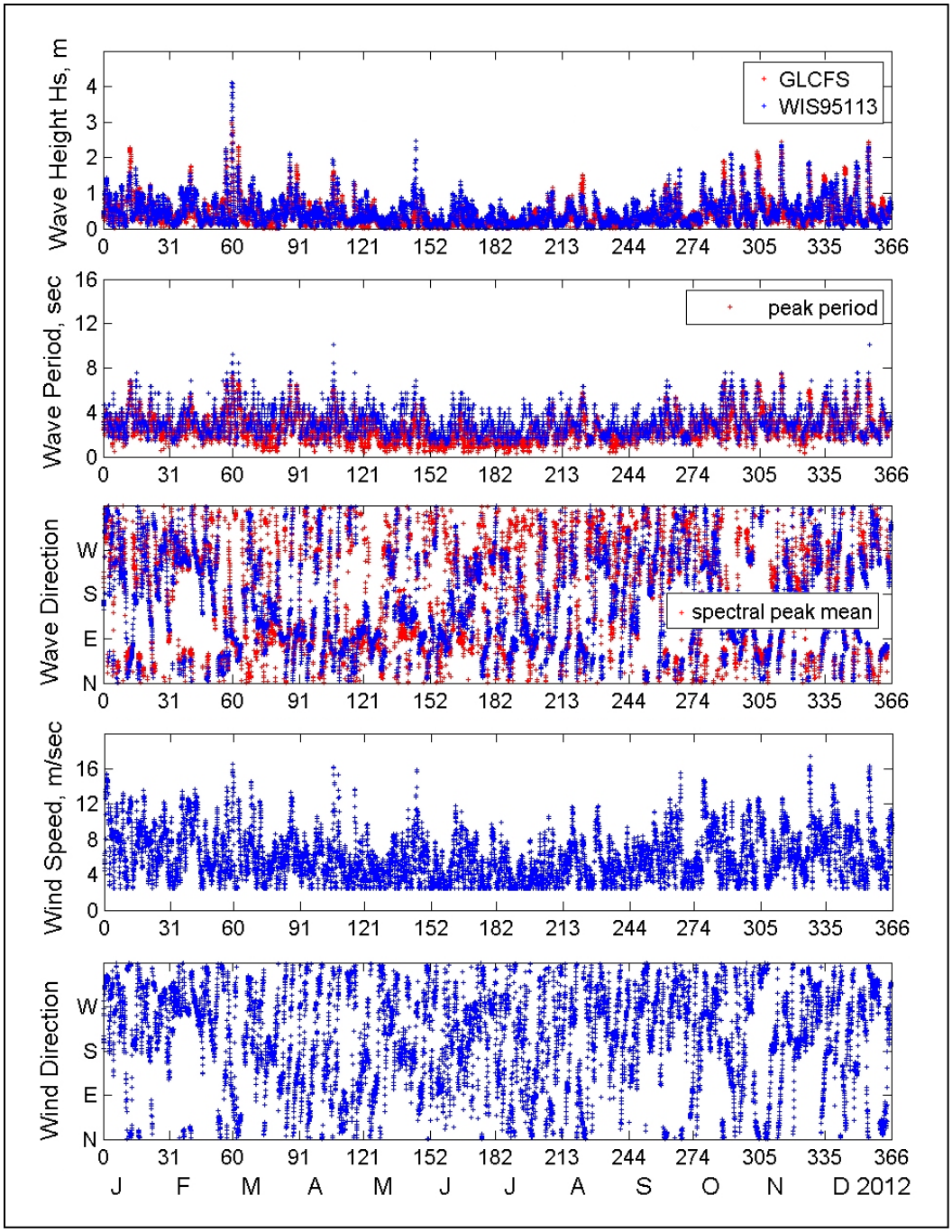

Figure 3-12. Comparison of GLCFS and WIS 2012 wind and wave data at WIS Sta 95113.

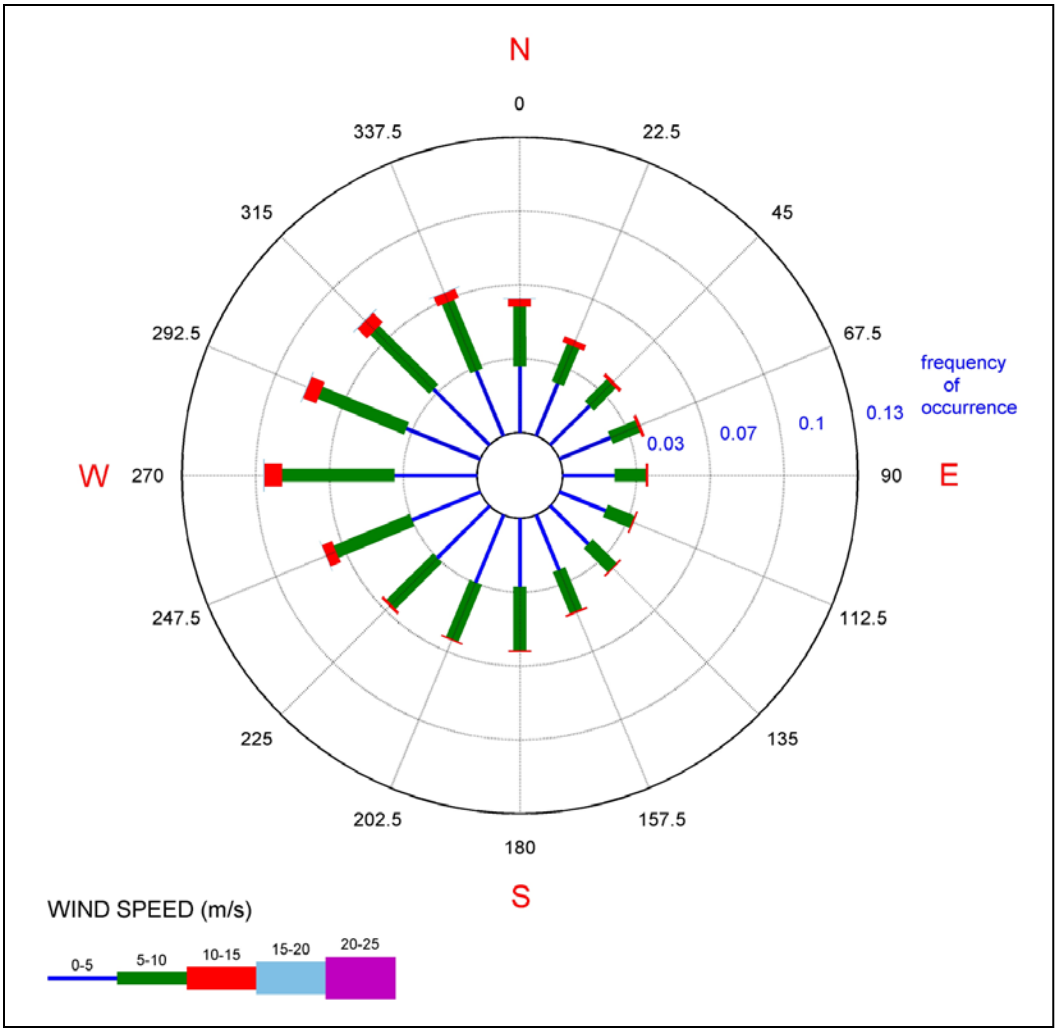

Figure 3-13. Wind roses at WIS Sta 95113 for 34-year hindcast data (1979-2012).

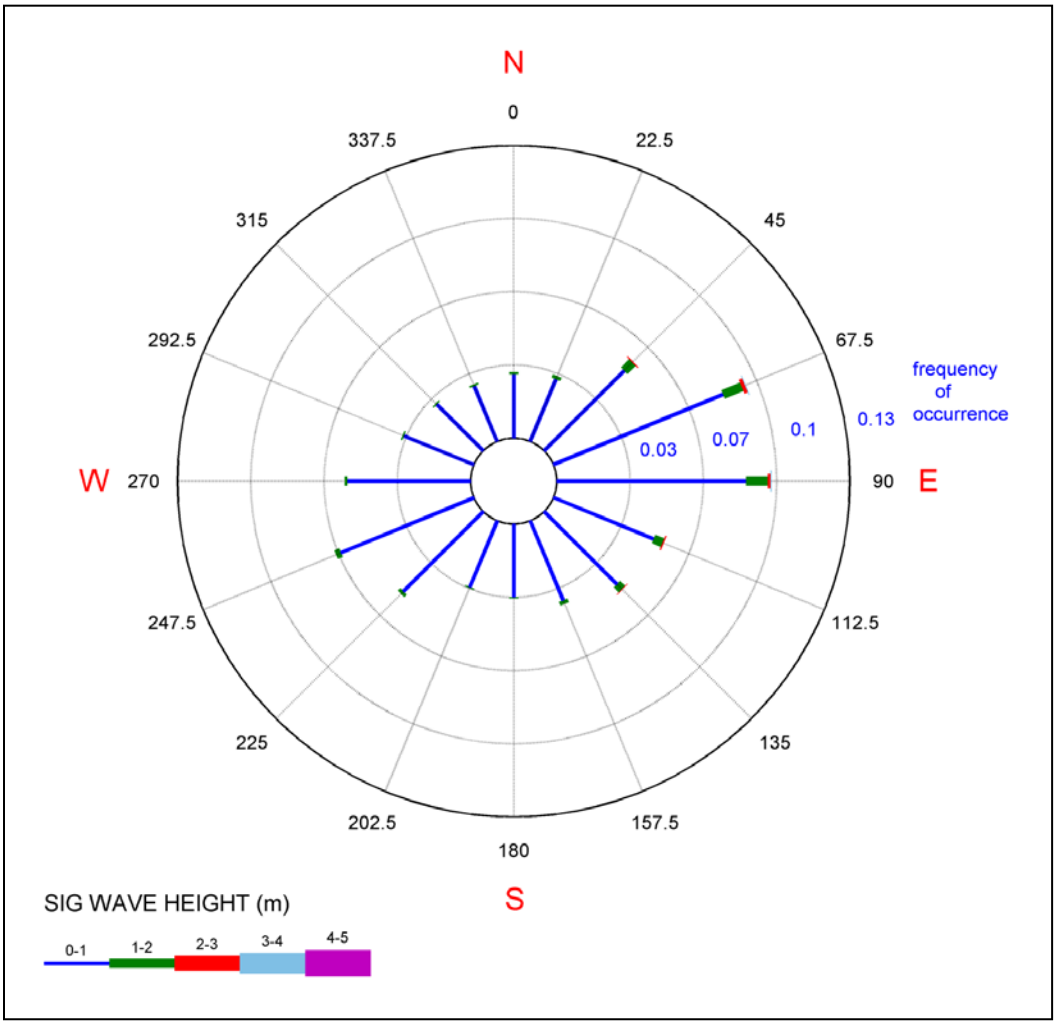

Figure 3-14. Wave roses at WIS Sta 95113 for 34-year hindcast data (1979-2012).

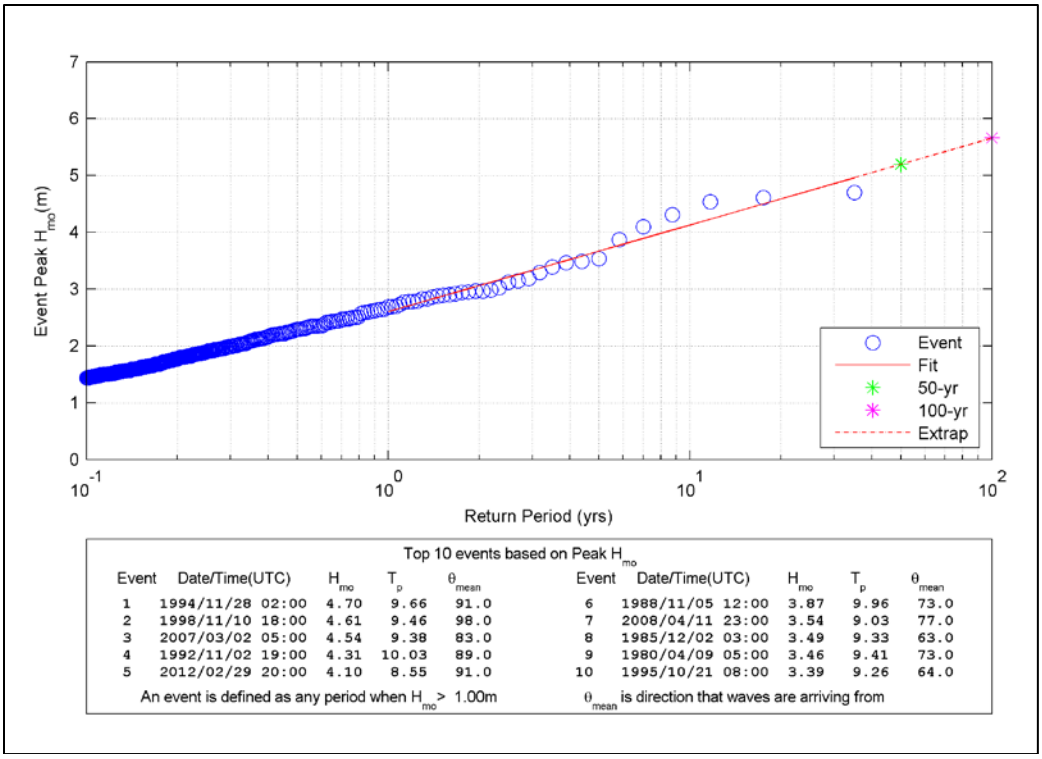

Figure 3-15. Analyzed extreme wave events at WIS Sta 95113.

Table 3-1. Non-storm wave simulation cases

Case	Year	Duration	CMS-Wave Grid	Configuration
1a	2008	1 May – 31 Aug	2008	Existing
1b	2008	1 Oct – 30 Nov	2008	Existing
2a	2009	1 May – 31 Aug	2008	Existing
2b	2009	1 Oct – 30 Nov	2008	Existing
3a	2010	1 May – 31 Aug	2010	Existing
3b	2010	1 Oct – 30 Nov	2010	Existing
4a	2011	1 May – 31 Aug	2011	Existing
4b	2011	1 Oct – 30 Nov	2011	Existing
5a	2012	1 May – 31 Aug	2011	Existing
5b	2012	1 Oct – 30 Nov	2011	Existing
6a	2013	1 May – 31 Aug	2013	Existing
6b	2013	1 Oct – 30 Nov	2013	Existing
6c	2013	1 May – 31 Aug	2013	Revetment
6d	2013	1 Oct – 30 Nov	2013	Revetment

Table 3-2. Storm wave simulation cases

Storm	Year	Duration	CMS-Wave Grid	Configuration
1a	2007	21 Feb – 6 Mar	2013	Existing
1b	2007	21 Feb – 6 Mar	2013	Revetment
2a	1985	11 Nov – 6 Dec	2013	Existing
2b	1985	11 Nov – 6 Dec	2013	Revetment
3a	1990	9 – 30 Oct	2013	Existing
3b	1990	9 – 30 Oct	2013	Revetment
4a	1992	27 Oct – 17 Nov	2013	Existing
4b	1992	27 Oct – 17 Nov	2013	Revetment
5a	1994	10 – 30 Nov	2013	Existing
5b	1994	10 – 30 Nov	2013	Revetment
6a	1995	11 – 28 Oct	2013	Existing
6b	1995	11 – 28 Oct	2013	Revetment
7a	1998	6 – 15 Nov	2013	Existing
7b	1998	6 – 15 Nov	2013	Revetment

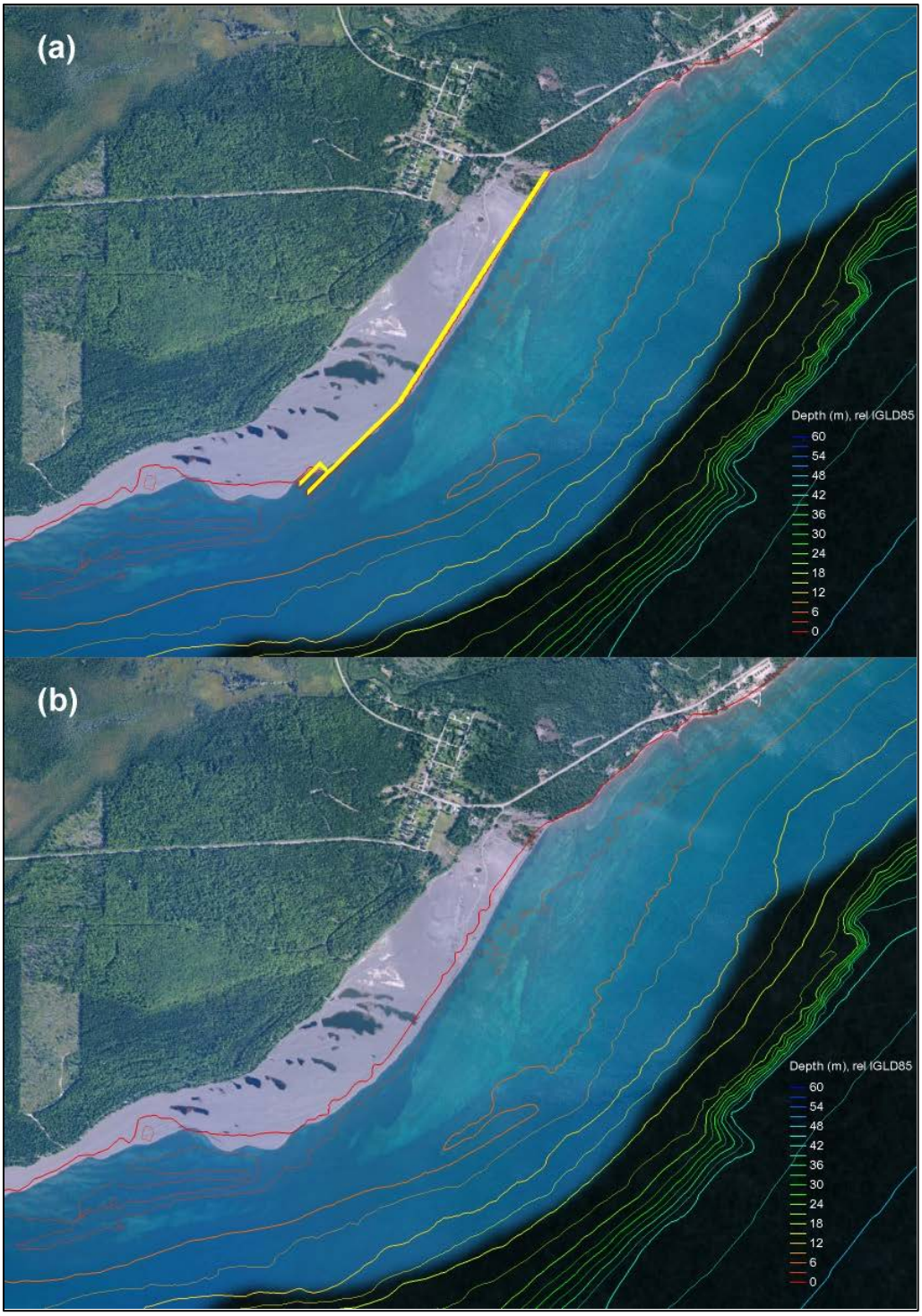

Figure 3-16. Depth Contours for (a) with revetment (yellow), and (b) existing configurations.

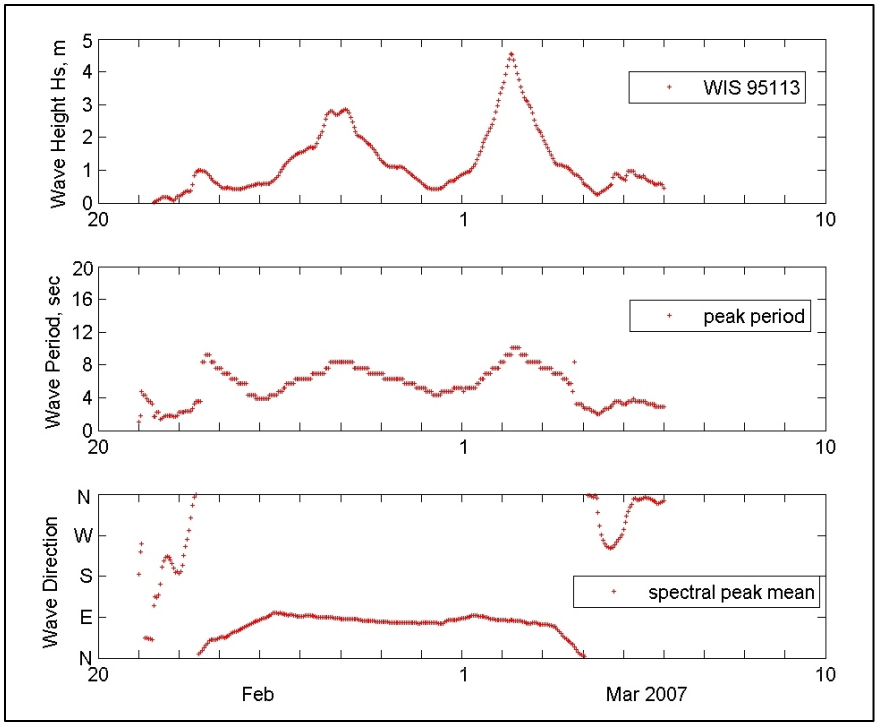

Figure 3-17. Time series of WIS data for Storm 1, 21 February – 6 March 2007.

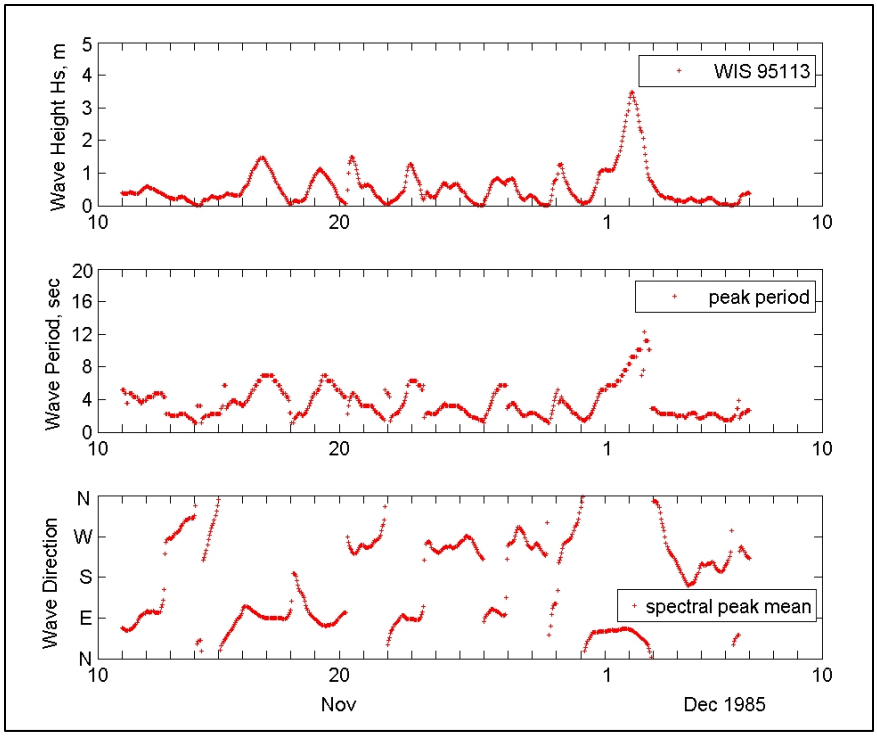

Figure 3-18. Time series of WIS data for Storm 2, 11 November – 6 December 1985.

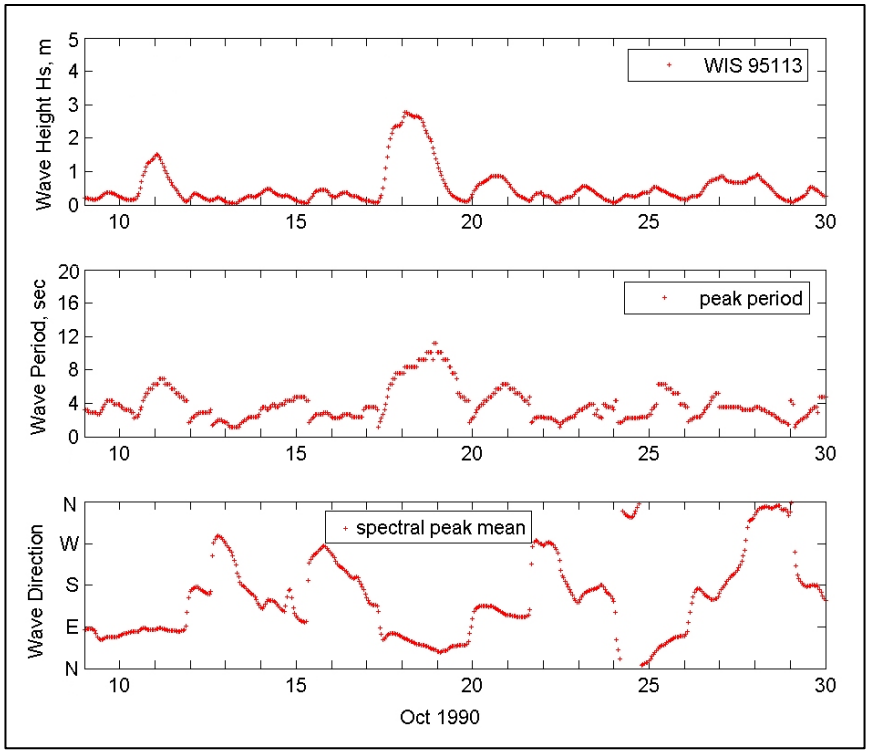

Figure 3-19. Time series of WIS data for Storm 3, 9-30 Oct 1990.

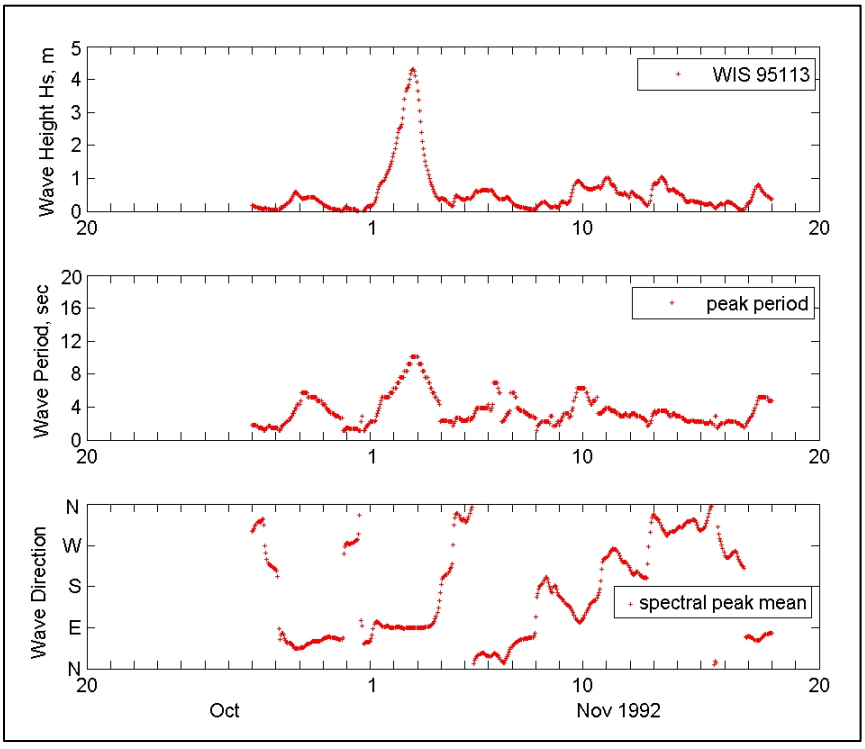

Figure 3-20. Time series of WIS data for Storm 4, 27 October – 17 November 1992.

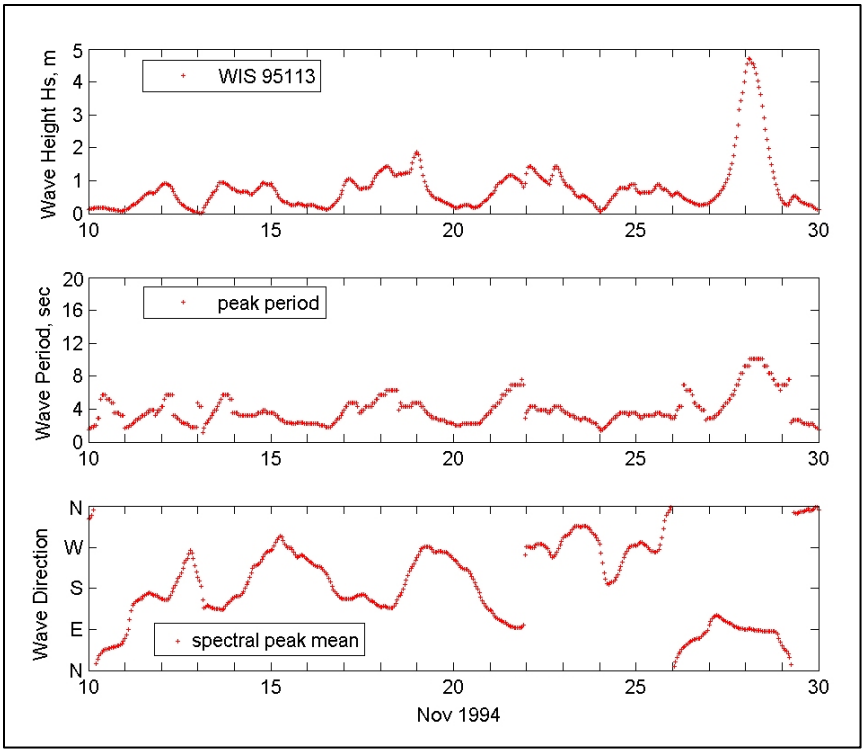

Figure 3-21. Time series of WIS data for Storm 5, 10 - 30 Nov 1994.

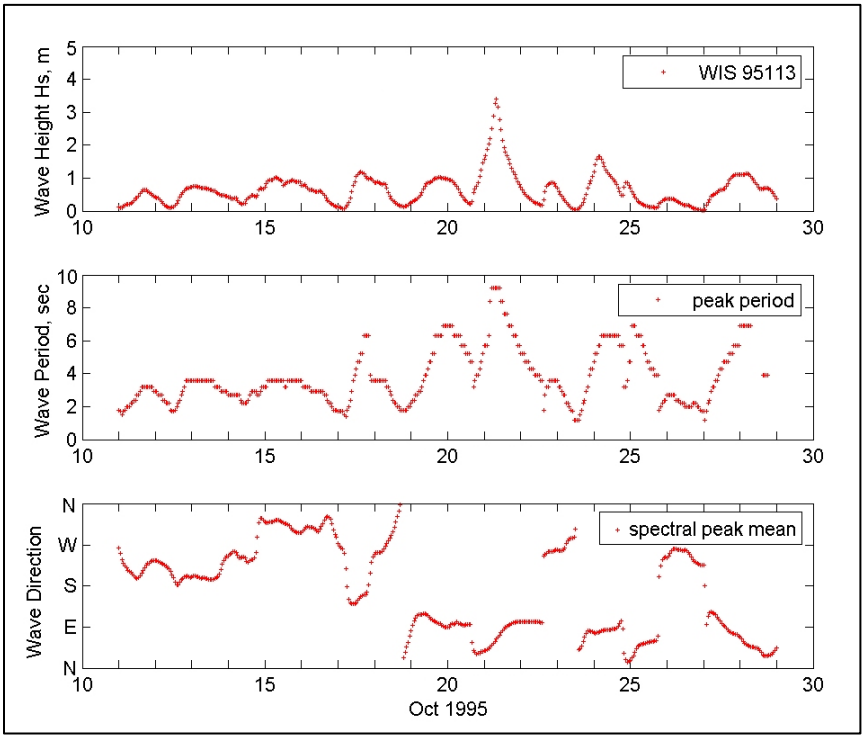

Figure 3-22. Time series of WIS data for Storm 6, 11 - 28 October 1995.

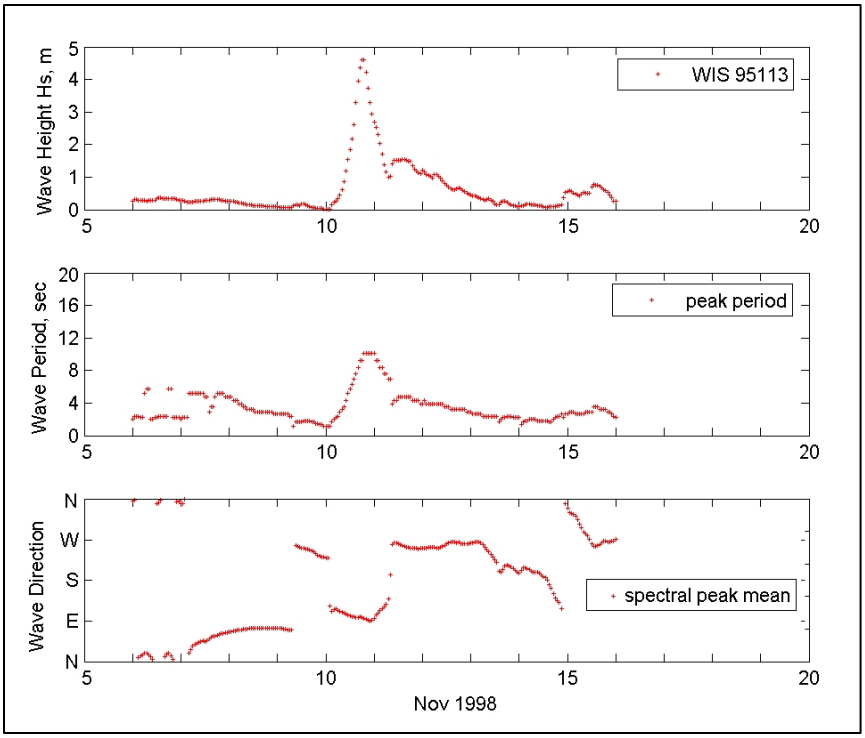

Figure 3-23. Time series of WIS data for Storm 7, 6 – 15 November 1998.

4 Sediment Transport Modeling

The sediment transport model in GSMB is the SEDZLJ sediment transport model (Jones and Lick 2001; James *et al*. 2010). SEDZLJ is an advanced sediment bed model that represents the dynamic processes of erosion, bedload transport, bed sorting, armoring, consolidation of fine-grain sediment dominated sediment beds, settling of flocculated cohesive sediment, settling of individual noncohesive sediment particles, and deposition. SEDZLJ is dynamically linked to CH3D-MB in that the hydrodynamics and sediment transport modules are run during each model time step. A description of SEDZLJ is given in Appendix A. SEDZLJ is not capable of simulating ice-induced sediment transport.

Setup of SEDZLJ

The SEDZLJ sediment model was setup to simulate sediment transport in the GSMB model domain seen in Figure 2-11 using the available sediment data (grain size distributions and specific gravities) for the Stamp Sands Deposits, Buffalo Reef, and the shoreline and surf zone along the shoreline between the deposits pile and Grand Traverse harbor. One of the first steps in performing sediment transport modeling is to use these data from the site to determine how many discrete sediment size classes are needed to adequately represent the full range of sediment sizes. Typically, five to eight size classes are used. For the current modeling study six size classes are used to represent the grain size distribution of the Stamp Sands, and six size classes are used to represent the native sediment. Each sediment size class is represented in SEDZLJ using the median or mean diameter within that size range. The six Stamp Sands sizes are 20, 188, 375, 750, 1,500, and 3,000 μm, and the six native sediment size classes are 20, 100, 188, 375, 750, and 3,000 μm. The classifications of the six Stamp Sands size classes are fine silt, fine sand, medium sand, coarse sand, very coarse sand, and very fine gravel. The classifications of the six native sediment size classes are fine silt, very fine sand, fine sand, medium sand, coarse sand, and very fine gravel. Based on the analysis of the sediment grab samples from the project site by ERDC-CHL, the specific gravities of the Stamp Sands and native sediment sediments used in the modeling are 2.90 and 2.65, respectively. The settling velocities for the seven different

sediment size classes were determined using Eq. A-2 (see Appendix A), and are shown in Table 4-1 below. The deposition rate for a particular size class was determined by multiplying the settling velocity by the suspended sediment concentration of that size class in the bottom layer. The probabilities of deposition for all size classes were set equal to one (Mehta 2014).

Table 4-1 Settling Velocities of Sediment Size Classes

Size Class	D_{50} (μm)	W_s (mm/s)
1	20	0.20
2	100	5.97
3	188	17.4
4	375	44.0
5	750	87.5
6	1,500	149.1
7	3,000	228.8

The erosion rates of the 12 sediment size classes were determined using the results obtained by Roberts *et al*. (1998) who measured the erosion rates of quartz particles in a SEDFLUME. SEDFLUME is a field- or laboratory-deployable flume for measuring the erosion rates of cohesive and noncohesive sediment beds (McNeil *et al*. 1996). The erosion rates for the five Stamp Sand size classes were adjusted by dividing the erosion rates given by Roberts *et al*. by the ratio 2.9/2.65, i.e., ratio of specific gravity of Stamp Sands to that of native sediment.

Spatially varying composition of the sediment bed in 18 of the 32 grid blocks in the Stamp Sands GSMB model (Figure 4-1) was specified for use as initial bed properties in SEDZLJ using all available sediment data. The grid blocks where spatially varying native sediment and the Stamp Sands compositions were specified in blocks 6-8, 10-12, 14-16, 18-20, 22-24, and 26-28 (see Figure 4-1). A non-erodible sediment bed was specified in the other 14 grid blocks. The reason for doing so is twofold: 1) no sediment data are available for these blocks; and 2) these blocks are far removed from Grand Traverse Bay, and thus even if sediment data were available

for these 14 grid blocks, simulating the erosion of sediment in these grid blocks would not have any impact on the sediment transport occurring in the other 18 grid blocks. Suspended sediment can be transported into these 18 blocks, and deposit on top of the non-erodible bed in low flow areas. Subsequently, these deposited sediments can be eroded if the bed shear stress in the cells where deposition occurred exceeds the critical shear stress for erosion specified for newly deposited sediments.

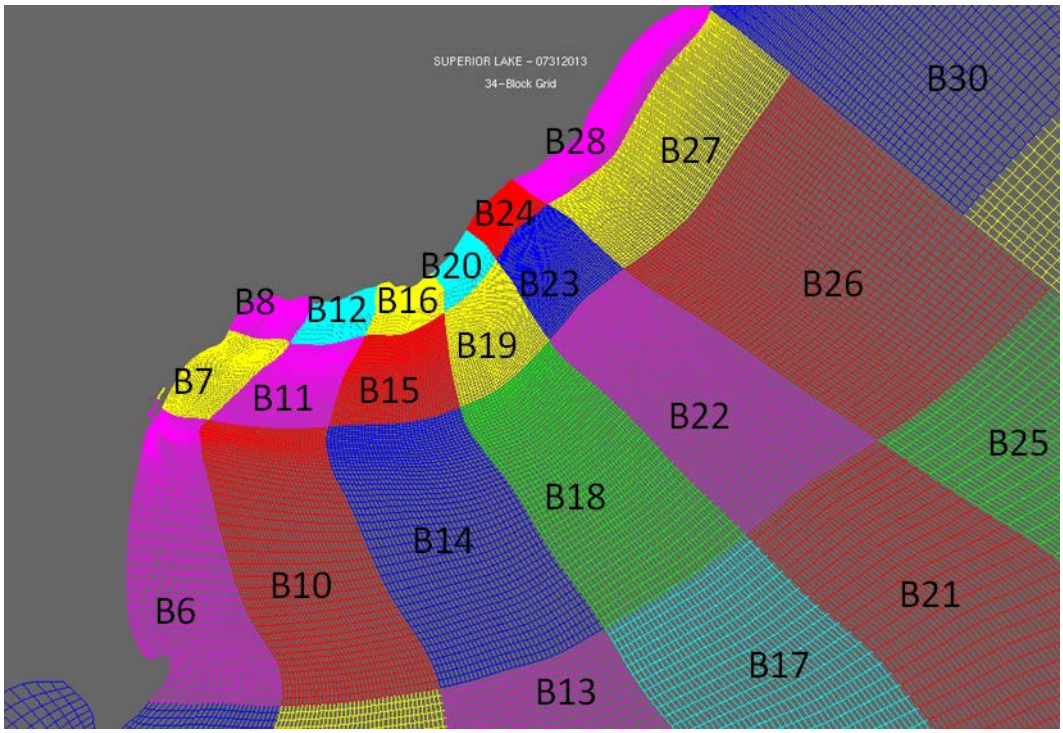

Figure 4-1. A portion of the 32 grid-block GSMB model domain

The sediment data used in specifying the initial bed compositions in the listed 18 grid blocks included the following:

- The previously mentioned grain size distributions and specific gravities determined from analysis of the collected sediment samples at the ERDC-CHL sedimentation laboratory.

- The substrate classifications in Grand Traverse Bay shown in Figure 4-2.

- As shown in Figure 4-3, the database that defines the existing spatial distribution of Stamp Sands on Buffalo Reef.

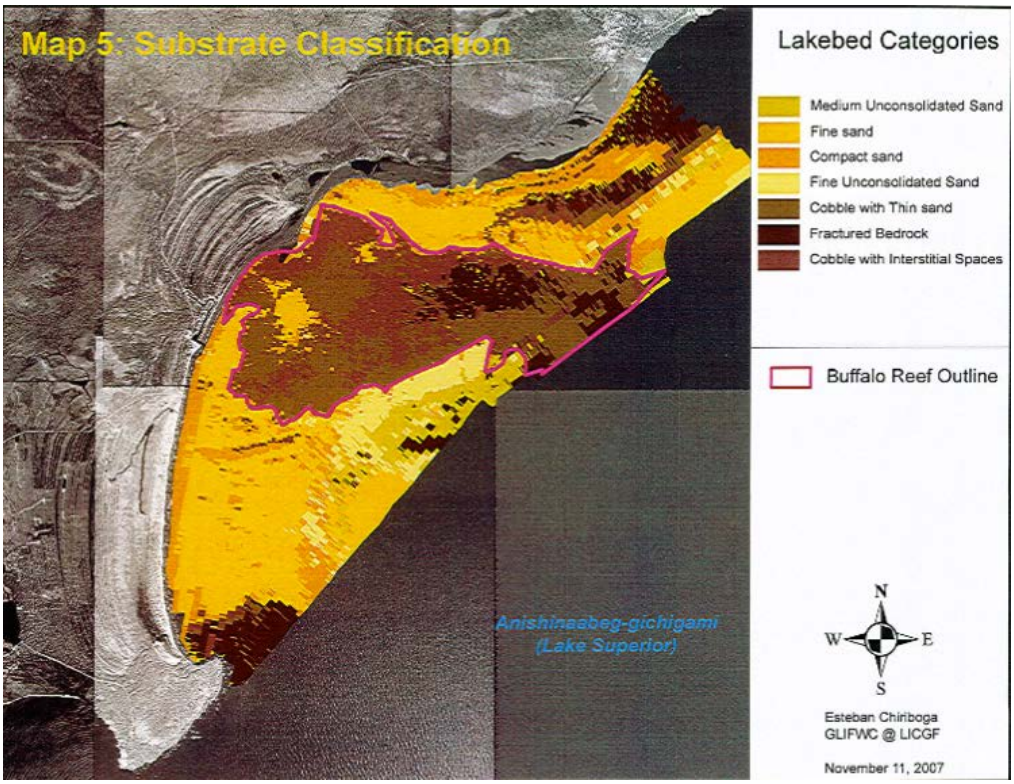

Figure 4-2. Substrate classifications in Grand Traverse Bay (after Chiriboga and Mattes 2008)

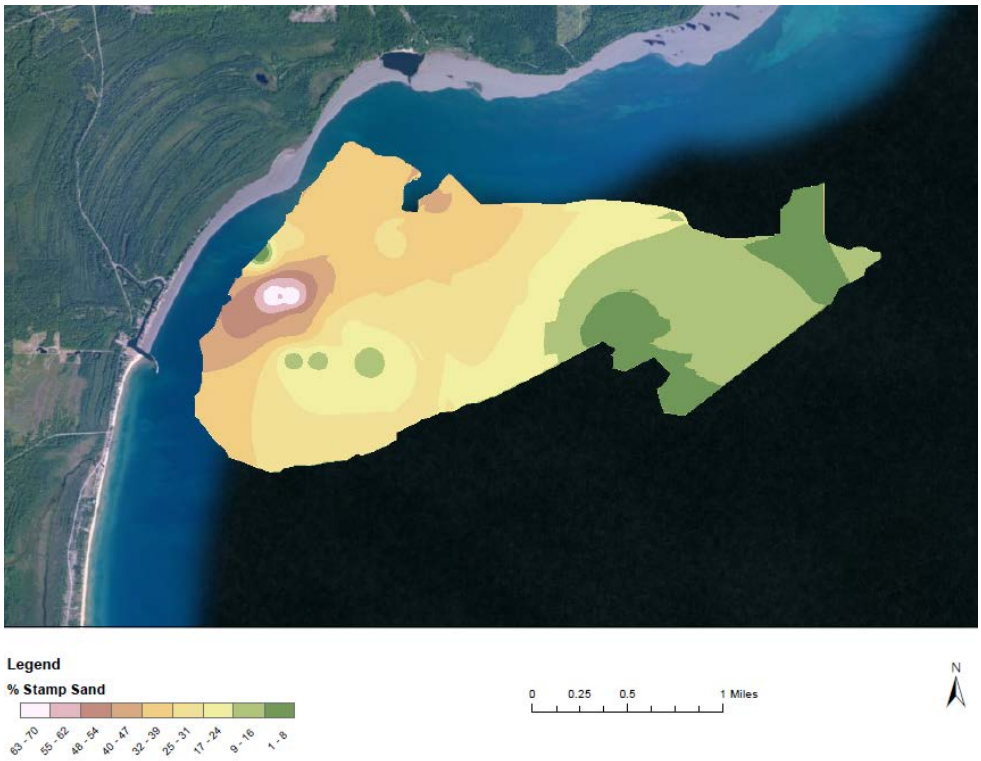

Figure 4-3. Spatial distribution of Stamp Sands on Buffalo Reef

All these data were combined and used to specify the spatially varying percentages of the 12 sediment size classes in the defined 18 grid blocks. The grain size distributions for the native sediment and for Stamp Sands sediment are shown in Table 4-2. Each number in this table represents the percentage of each of the 12 sediment size classes for the two sediment types in the top bed layer. The first two size classes shown in this table represent medium size silts for native sediment and Stamp Sands, respectively. As shown, there are 3 percent silt size sediment in the average native sediment grain size distributions (GSD) and 2 percent in Stamp Sands GSD. Classes 3 – 7 represent the percentages of 100, 188, 375, 750, and 3,000 μm size classes in the native sediment GSD, and Classes 8 – 12 represent the percentages of 188, 375, 750, 1,500, and 3,000 μm size classes in the Stamp Sands GSD.

Table 4-2 Percentages of Sediment Size Classes for Sediment Types

Sediment Type	Sediment Size Class											
	1	2	3	4	5	6	7	8	9	10	11	12
Native Sediment	3	0	17	40	20	10	10	0	0	0	0	0
Stamp Sands	0	2	0	0	0	0	0	3	12	58	20	5

Next, the spatial distribution of Stamp Sands on Buffalo Reef shown in Figure 4-3 was interpolated onto the grid blocks that represent Buffalo Reef. The grain size distribution in each grid cell that is inside the boundaries of Buffalo Reef was adjusted by the calculated percentage of Stamp Sands in those cells. For example, if the interpolated percentage of Stamp Sands in a certain cell was 25 percent, then the grain size distribution in that cell was adjusted so that it was composed of 25 percent Stamp Sands and 75 percent native sediment. So the percentages of the 12 sediment size classes in that cell were set equal to the following:

(SC1,SC3,SC4,SC5,SC6,SC7)*0.75 + (SC2,SC8,SC9,SC10,SC11,SC12)*0.25

where SC = sediment class.

The existing sediment bed in each grid cell was divided into four vertical layers (see Figure A-2). The assumption was made that the initial distribution of the 12 size classes, bulk densities, and gross erosion rates are the same in all four bed layers, *i.e.*, there is no initial vertical stratification of sediment grain sizes, bulk densities or erosion rates that normally result from the repetitive processes of deposition, erosion, and armoring of the top bed layer.

Kerfoot *et al.* (2???) have found that the Stamp Sands pile is retreating at an average rate of 26 ft/year (7.9 m/yr). This source of Stamp Sands was added to the active model grid using the following approximation method. The volume, V, of sand that is added to the surf zone in front of the pile each year was estimated by multiplying the length of the pile by the estimated average height by 26 ft; $V \sim 67{,}000$ CY. The width of the surf zone was approximated to be four grid cells, which is approximately 40 m. Since approximately 6.5 months per year was simulated (May-August + October-November + one storm), the rate at which Stamp Sands was added to the surf zone was calculated as

$$\dot{V} = \frac{V}{15{,}768{,}000}\frac{\Delta\ell}{L}$$

where L = length of Stamp Sands pile, $\Delta l \simeq 25$m = average length of cells in front of the Stamp Sands pile, Δt = time step = 2 sec, and where 15,768,000 = number of seconds in six months, *i.e.*, it was not added during the simulated storm event. To increase computational efficiency, the volume of sand eroded from the pile per second was added to the four surf zone grid cells once per day. The volume of Stamp Sands that was added to each of the four cells per day is given by

$$Volume = \frac{\dot{V} * 86{,}400}{4 * \Delta t}$$

where Δt = model time step = 2 sec, and 86,400 = number of seconds per day. This sediment volume was converted to sediment mass, and was then added to layer 2 in the SEDZLJ layered bed model since new deposits are automatically added to the second layer. The calculated mass was distributed into the six grain size classes that were used to represent Stamp Sands. The percentages of fine silt, fine sand, medium sand, coarse

sand, very coarse sand, and very fine gravel sediment classes that the sediment mass added to each of the surf zone grid cells once per day are divided into are 2, 3, 12, 58, 20, and 5 percent, respectively.

Model Calibration and Validation

The sediment transport model in GSMB was calibrated and partially validated using morphological changes calculated from LiDAR surveys of Grand Traverse Bay there were performed in 2008, 2010, 2011, and 2013. The steps performed in these analyses are described below.

- The spatial data in each one of the LiDAR surveys were interpolated onto the grid blocks that fell within the shoreline and offshore area that was surveyed in the specified years. Differences in the morphology from, for example, 2010 to 2011, were obtain by subtracting the bed elevations in the grid blocks that contain the 2010 and 2011 surveys. This difference in bed elevation approximates the net change in the offshore and alongshore movement of both native sediment and Stamp Sands at the project site in the time interval between LiDAR surveys.

- Calibration of the sediment transport model in GSMB was conducted by comparing the morphologic differences between LiDAR surveys conducted in 2010 and 2011 to morphologic differences simulated by GSMB. The following three time periods were modeled:

  April – August 2010: The 2010 LiDAR survey data were used for the initial morphology for this model simulation (Case 3a in Table 2-1). The simulation during April 2010 was used to spin-up the hydrodynamic model. The sediment transport model was started on May 1, and it was run for four months (May 1 – August 31).

  September – November 2010: The morphology at the end of the April – August 2010 model simulation was used as the initial morphology for this model run (Case 3b in Table 2-2). The simulation during September 2010 was used to spin-up the hydrodynamic model. The sediment transport model was started on October 1, and it was run for two months (October 1 – November 30). The currents in the project area are generally higher during these two months than the other ice-free months, so more sediment is transported during these two months than during the fairer weather that occurs during May through August.

Storm Event: One of the storm events listed in Table 2-2 was randomly selected for simulation following the simulation of Case 3b. The purpose of this third simulation was to include a single storm (i.e., higher energy event) into each year's simulation. It is recognized that in most years, more than one higher energy event probably occurs on Lake Superior, but including one storm per 'year' in the calibration and validation model runs allows for more realism in the model results. The randomly selected storm for the calibration run was Storm 2 (see Table 2). The morphology at the end of the September – November 2010 model simulation was used as the initial morphology for this model run.

- The morphology at the end of these three model runs was subtracted from the initial morphology (i.e., at the start of the April – August 2010 model simulation) and then compared with the morphological difference. If the average differences found between the surveys and model results in the different regions (e.g., different parts of Buffalo Reef, the trough, along the shoreline downdrift of the Stamp Sands pile) of the model domain were found to be greater than 25 percent, the spatial pattern of the differences were examined and appropriate changes made in the model parameterization of the sediment transport processes that control morphologic changes in those areas.

- The calibrated sediment transport model was partially validated by comparing morphologic differences between the LiDAR surveys conducted in 2008 and 2010 to the morphologic differences simulated by GSMB. The following six time periods were modeled:

  April – August 2008: The 2008 LiDAR survey data were used for the initial morphology for this model simulation (Case 1a in Table 2-1). The simulation during April 2008 was used to spin-up the hydrodynamic model. The sediment transport model was started on May 1, and it was run for four months (May 1 – August 31).

  September – November 2008: The morphology at the end of the April – August 2008 model simulation was used as the initial morphology for this model run (Case 1b in Table 2-2). The simulation during September 2008 was used to spin-up the hydrodynamic model. The sediment transport model was started on October 1, and it was run for two months (October 1 – November 30).

Storm Event: One of the storm events listed in Table 2-2 was randomly selected for simulation following the simulation of Case 1b. The randomly selected storm for this calibration run was Storm 4 (see Table 2-2). The morphology at the end of the September – November 2008 model simulation was used as the initial morphology for this model run.

April – August 2009: The morphology at the end of the 2008 Storm Event was used for the initial morphology for this model simulation (Case 2a in Table 2-1). The simulation during April 2009 was used to spin-up the hydrodynamic model. The sediment transport model was started on May 1, and it was run for four months (May 1 – August 31).

September – November 2009: The morphology at the end of the April – August 2009 model simulation was used as the initial morphology for this model run (Case 2b in Table 2-2). The simulation during September 2009 was used to spin-up the hydrodynamic model. The sediment transport model was started on October 1, and it was run for two months (October 1 – November 30).

Storm Event: One of the storm events listed in Table 2-2 was randomly selected for simulation following the simulation of Case 1b. The randomly selected storm for the calibration run was Storm 1 (see Table 2-2). The morphology at the end of the September – November 2009 model simulation was used as the initial morphology for this model run.

- The morphology at the end of these six model runs was subtracted from the initial morphology (*i.e.*, at the start of the April – August 2008 model simulation) and then compared with the difference between the 2008 and 2010 LiDAR surveys. When the average differences found between the surveys and model results in the different regions (*e.g.*, different parts of Buffalo Reef, the trough, along the shoreline downdrift of the Stamp Sands pile) of the model domain were found to be greater than 25 percent, the spatial pattern of the differences were examined and appropriate changes made in the model parameterization of the sediment transport processes that control morphologic changes in those areas.

Model Simulations

The calibrated and partially validated GSMB model results were used to develop an approximate 10-year sediment prediction of how much more of Buffalo Reef will be covered by Stamp Sands for both the without-project and with-project conditions. As stated previously, approximately 25 percent of Buffalo Reef is currently covered. The model simulations that were performed are described in this section, and the analysis of the model results is described in the next chapter.

The morphology at the project site determined from the 2013 LiDAR survey was used for the initial bathymetry and shoreline geometry for both the without-project and the with-project model simulations. As described in Section 1, the with-project condition includes a 6,600 ft (2,012 m) rubble mound revetment in front of the original pile of Stamp Sand deposits (see Figure 1-6), and the without-project condition is the 2013 shoreline measured by the LiDAR survey. Figures 4-4 and 4-5 show the without-project and the with-project grids along the length of the Stamp Sands pile, respectively. The LiDAR surveyed shoreline downstream of the Stamp Sands pile was used for the area downdrift of the transfer area (see Figure 4-5b).

To develop the 10-year estimate for the increase in coverage of Buffalo Reef with Stamp Sands, the 19 model simulations shown in Table 4-3 were performed for both scenarios, *i.e.*, without-project and with-project. The Case numbers refer to the simulated events shown in Tables 2-1 and 2-2, with "S" added in front of the storm number shown in Table 2-2. No dates are given in Table 4-3 for the seven storms simulated since they were represented as separate events. The 19 model runs for both scenarios were considered to represent an approximate six year sediment transport simulation. The average annual net change in morphology was calculated by determining the difference in morphology from that which existed at the end of the 19th model run to the initial morphology used for the first model run (*i.e.*, Case 1a) and dividing that difference for each grid cell by six. This difference was extrapolated for the remaining four years by sequentially adding the average annual morphological difference onto the morphology that existed at the end of the 19th model run. The results of this analysis are given in the next chapter.

Figure 4-4. Without-Project Grid in Proximity to the Stamp Sands Pile

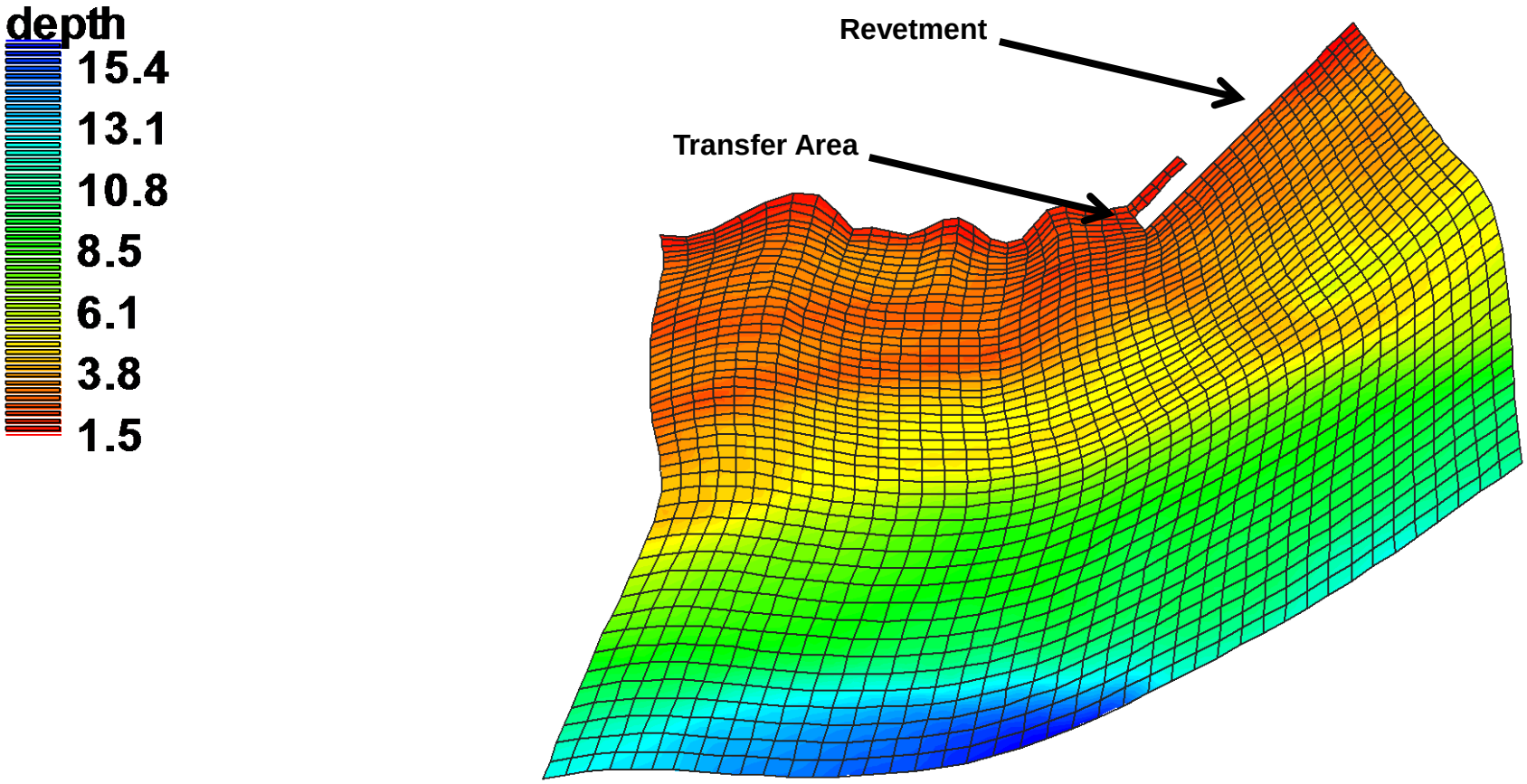

Figure 4-5a. With-Project Grid in Proximity to the Southern End of the Stamp Sands Pile

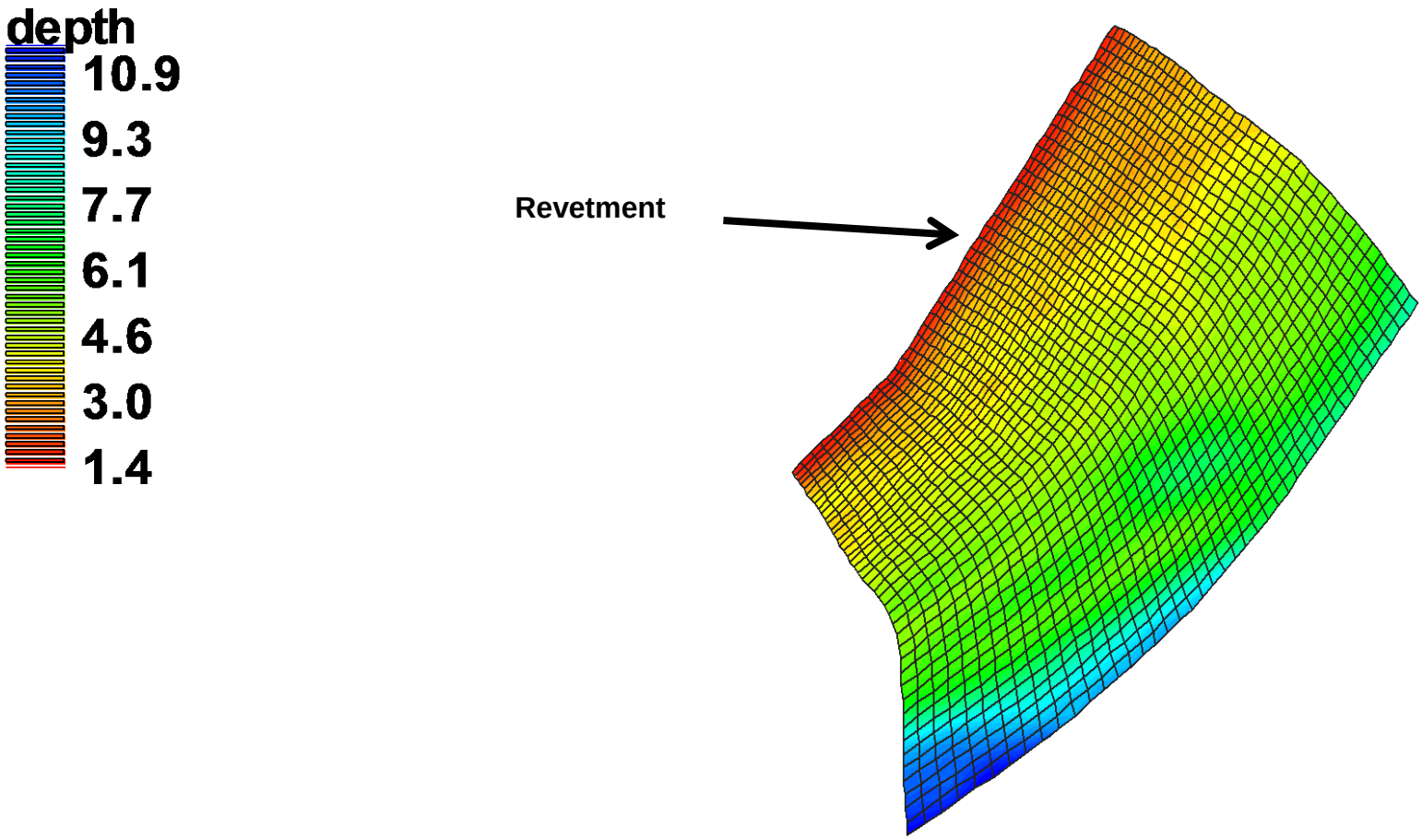

Figure 4-5b. With-Project Grid in Proximity to the Northern End of the Stamp Sands Pile

Table 4-3 Simulations Performed for With-Project and Without-Project Conditions

Case	Initial Bathymetry/Geometry	Time Period
1a	2013 LiDAR Survey data	1 Apr – 31 Aug
1b	Output from 1a	1 Sep – 30 Nov
S6	Output from 1b	-
2a	Output from S7	1 Apr – 31 Aug
2b	Output from 2a	1 Sep – 30 Nov
S3	Output from 2b	-
3a	Output from S3	1 Apr – 31 Aug
3b	Output from 3a	1 Sep – 30 Nov
S1	Output from 3b	-
4a	Output from S1	1 Apr – 31 Aug
4b	Output from 4a	1 Sep – 30 Nov
S5	Output from 4b	-
5a	Output from S5	1 Apr – 31 Aug
5b	Output from 5a	1 Sep – 30 Nov
S4	Output from 5b	-
6a	Output from S7	1 Apr – 31 Aug
6b	Output from 6a	1 Sep – 30 Nov
S2	Output from 6b	-
S7	Output from S2	-

5 Modeling Results

Analysis of Sediment Transport Modeling Results

The comparison of the with-project and without-project simulations described in Chapter 4 provided insight as to whether the rubble mound revetment alternative, i.e., the with-project alternative, would satisfy the intended purpose of minimizing the offshore transport of the Stamp Sand sediments onto Buffalo Reef as well as their ongoing longshore transport. The 10-year estimates of the continued longshore and offshore spread of the Stamp Sands for both alternatives are shown below in Figures 5-1 – 5-4.

Figure 5-1 is a color contour plot of the estimated 10-year net change in bathymetry for the without-project alternative. This figure shows the entire offshore area where the change in morphology due to the net-erosion and net-deposition was calculated. As described in the last chapter, this area represents 18 of the 32 grid blocks used in the GSMB modeling. The green to dark blue represents areas of net-deposition, whereas the yellow to red represents areas of net-erosion. Figure 5-2 shows the same results as Figure 5-1, but it is zoomed into Buffalo Reef (the outline of which is shown by the dark lines) and a line contour plot was used instead of a color contour one so that the outline of Buffalo Reef could be seen. In addition, the scale on the contour plot was restricted from -25 to 25 inches to be able to see more detail of the morphological changes on Buffalo Reef.

Figure 5-3 is a color contour plot of the estimated 10-year net change in bathymetry for the with-project alternative. As in Figure 5-1, this figure shows the entire offshore area where the change in morphology due to the net-erosion and net-deposition was calculated. The green to dark blue represents areas of net-deposition, whereas the yellow to red represents areas of net-erosion. Figure 5-4 shows the same results as Figure 5-3, but it is zoomed into Buffalo Reef (the outline of which is shown by the dark lines) and a line contour plot was used instead of a color contour one so that the outline of Buffalo Reef could be seen.

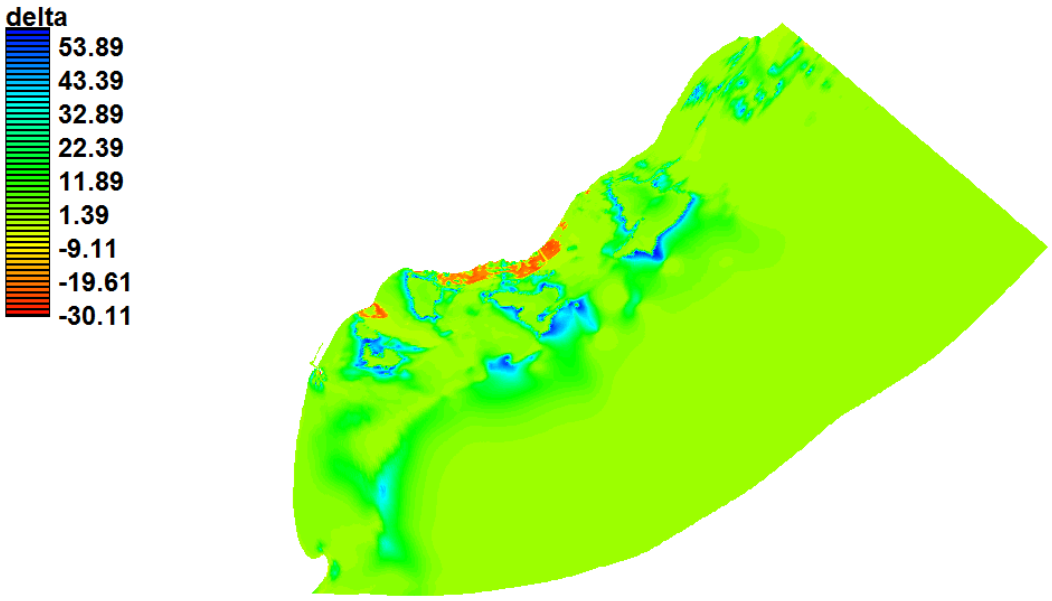

Figure 5-1. 10-Year Net Change in Bathymetry in the 18 Morphologically Active Grid Blocks for the Without-Project Alternative.

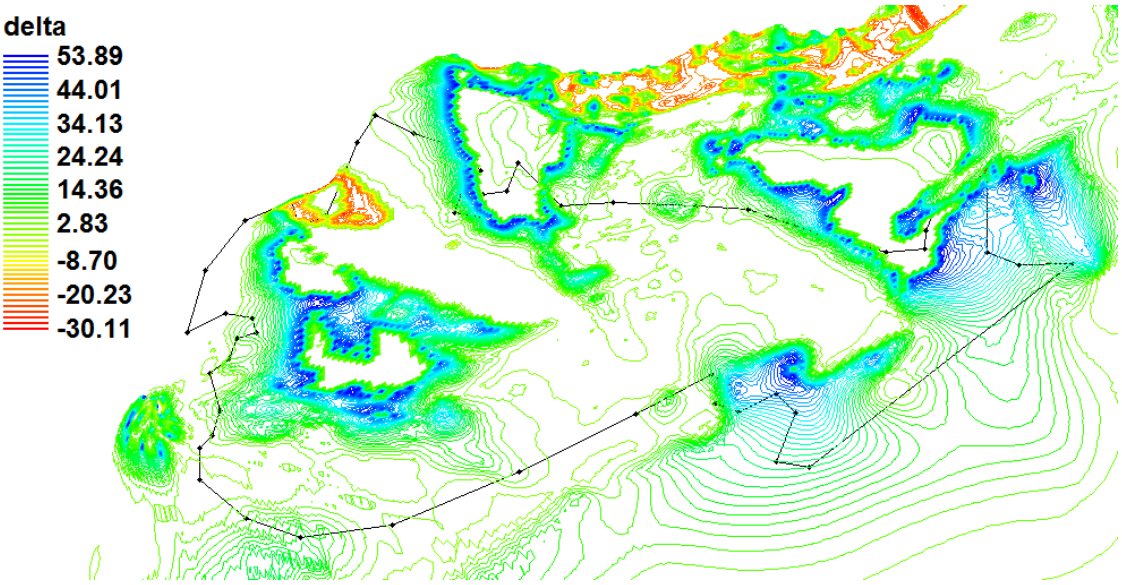

Figure 5-2. 10-Year Net Change in Bathymetry in the Buffalo Reef area for the Without-Project Alternative.

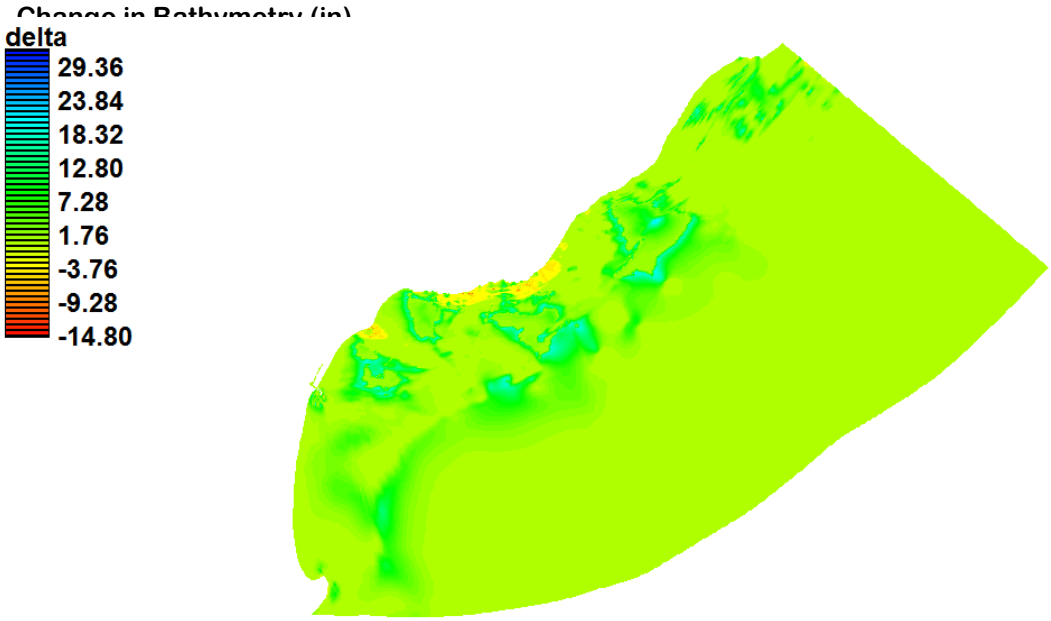

Figure 5-3. 10-Year Net Change in Bathymetry in the 18 Morphologically Active Grid Blocks for the With-Project Alternative.

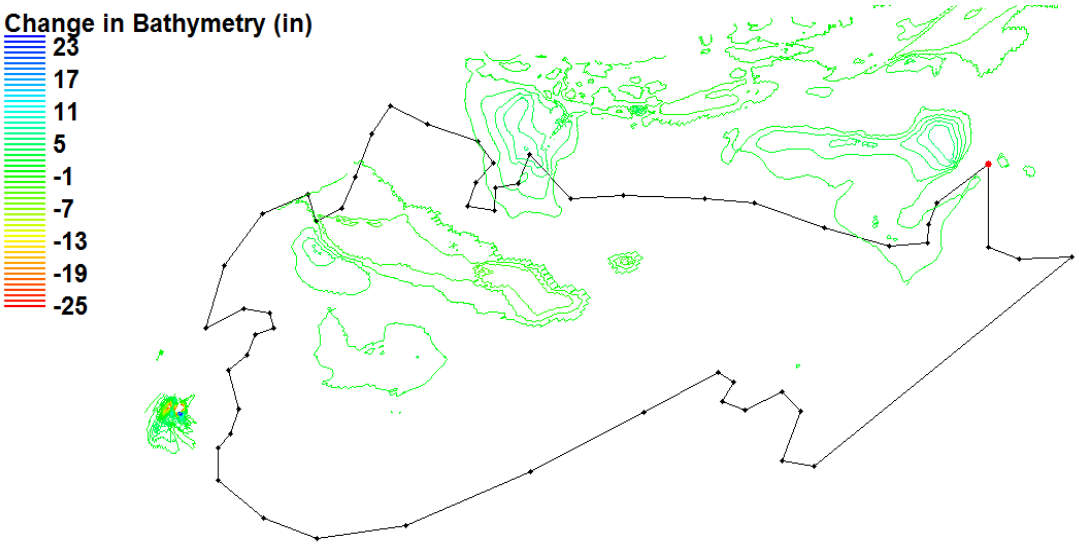

Figure 5-4. 10-Year Net Change in Bathymetry in the Buffalo Reef area for the With-Project Alternative.

Percentages of Buffalo Reef that were covered with at least one inch (2.54 cm) of Stamp Sands for both alternatives were determined. For the without-project alternative, an estimated 60 percent of Buffalo Reef (net increase of 35 percent) will be covered by at least one inch over the next 10 years. Even for the with-project alternative, *i.e.*, with the proposed rubble-mound revetment, Stamp Sands already in the littoral zone will continue to move downdrift towards Buffalo Reef and Grand Traverse harbor. As a result, an estimated 35 percent of Buffalo Reef (net increase of 10 percent) will be covered by at least one inch of Stamp Sands for the with-project alternative. Both these above reported percentages include the existing 25 percent coverage. The other estimate of interest that was calculated from the 10-year estimates developed for both project alternatives are that the average sedimentation rates in the natural trough (see Figure 1-5) that borders the updrift side of Buffalo Reef are approximately 30,000 CY and 10,000 CY, respectively for the without-project and with-project alternatives.

Conceptual Site Model

The conceptual site model (CSM) for the existing (*i.e.*, without-project) system developed from an analysis of the available data as well as the results from the sediment transport modeling indicate that Stamp Sands that are eroded from the main pile enter the littoral zone in front of the pile (approximately 65,000 CY/year), and are subsequently transported mostly in the longshore (i.e., downdrift) direction (about 55,000 CY), with about 10,000 CY being transported offshore during high energy events. The areas offshore where the Stamp Sands deposit are the darker blue areas seen in Figure 5-1. Approximately 30,000 CY of the eroded sediments that are transported longshore deposit in the trough, and approximately 8,000 CY gets transported onto Buffalo Reef, and the remainder (approximately 17,000 CY) is transported further longshore down towards Grand Traverse Harbor. There does not appear to be a single dominant path by which the Stamp Sands get transported to Buffalo Reef. A small fraction of the sediment that gets transported to and deposits on Buffalo Reef gets resuspended and transported further offshore during storm events.

The CMS for the with-project alternatives mostly differs because the source is cutoff by the rubble mound revetment. The Stamp Sands already in the littoral zone in front of the revetment get transported in the down

drift direction by the longshore currents during non-storm conditions and offshore as well during storm events. The estimated 10-year sediment budget shows that approximately 10,000 CY of Stamp Sands deposit in the trough, and only approximately 1,500 CY gets transported onto Buffalo Reef. Of course, the quantity of Stamp Sands that gets transported onto Buffalo Reef will decrease with time as the quantity of Stamp Sands in the littoral zone decreases due the source (i.e., Stamp Sands pile) being eliminated in the with-project alternative. Extrapolation beyond 10-years to determine the rate of decrease was not performed as it would have a very high uncertainty associated with such an estimate.

6 Conclusions

Model simulations of the transport of Stamp Sands along the Keweenaw Peninsula shoreline downdrift of the Gay, MI Stamp Sands main deposit as well as offshore onto Buffalo Reef were performed using the GSMB numerical hydrodynamic and mixed sediment transport model. Specifically, the GSMB sediment transport model was used to predict the future spread of the Stamp Sands deposits (both longshore and offshore) as well as the impact of the following two alternative management actions: 1) a without-project alternative (which is the existing condition); and 2) a with-project condition that included a shoreline parallel 6,600 linear ft rubble mound revetment that would serve as a barrier between the main Stamp Sand deposit and the shoreline and littoral zone in front of the proposed revetment. The model simulations of both alternatives were used to develop a ten-year sediment budget that allowed for the percentage of Buffalo Reef that was covered with at least one inch (2.54 cm) of Stamp Sands for both alternatives to be determined. The initial condition used for both simulations was that Buffalo Reef is currently 25 percent covered by Stamp Sands.

For the without-project alternative, an estimated 60 percent of Buffalo Reef will be covered by at least one inch of Stamp Sands over the next 10 years. For the with-project alternative, *i.e.*, with the proposed rubble-mound revetment, Stamp Sands already in the littoral zone will continue to move downdrift towards Buffalo Reef and Grand Traverse Harbor. As a result, an estimated 35 percent of Buffalo Reef will be covered by at least one inch of Stamp Sands for the with-project alternative. This comparison of the model simulations for the with-project and without-project alternatives simulations showed that the proposed rubble mound revetment alternative would satisfy the intended purpose of minimizing the offshore transport of these contaminated sediments onto Buffalo Reef as well as their ongoing longshore transport.

References

Arega, F., and E.J. Hayter. 2008. “Coupled consolidation and contaminant transport model for simulating migration of contaminants through sediment and a cap.” Journal of Applied Mathematical Modelling, 32:2413–2428.

Bunch, B. W., Channel, M., Corson, W.D., Ebersole, B.A., Lin, L., Mark, D. J., McKinney, J.P., Pranger, S.A., Schroeder, P.R., Smith, S.J., Tillman, D.H., Tracy, B.A., Tubman, M.W., and Welp, T.L. 2003. “Evaluation of Island and Nearshore Confined Disposal Facility Alternatives, Pascagoula River Harbor Dredged Material Management Plan,” Technical Report ERDC-03-3, U.S. Army Engineer Research and Development Center, Vicksburg, MS.

Cerco, C., and T. Cole. 1994. “Three-Dimensional Eutrophication Model of Chesapeake Bay,” Technical Report EL-94-4, US Army Engineer Waterways Experiment Station, Vicksburg, MS.

Chapman, R.S., B.H. Johnson, and S.R. Vemulakonda. 1996. “User guide for the sigma stretched version of CH3D-WES; A three-dimensional numerical hydrodynamic, salinity and temperature model.” Technical Report HL-96-21, U.S. Army Engineer Waterways Experiment Station, Vicksburg, MS.

Chapman, R.S., P.V. Luong, and M.W. Tubman. 2006. “Mississippi Sound hydrodynamic and salinity sensitivity modeling.” Final Report prepared for U. S. Army District, Mobile, AL.

Chapman, R. S., and P.V. Luong. 2009. “Development of a multi-block CH3D with a wetting, drying and CLEAR linkage capability.” Draft Report prepared for Louisiana Coastal Area (LCA) Ecosystem Restoration Plan S&T Office, Vicksburg, MS.

Chapman, R.S., K.J. Eisses, and T.O. McAlpin. 2010. “Numerical modeling studies supporting Port of Anchorage deepening and expansion; part iii: numerical hydrodynamic modeling,” Proceedings 11th International Conference on Estuarine and Coastal Modeling; November 4-6, 2010, Seattle, WA, 301-316.

Chapman, R.S., A.S. Grzegorzewski, P.V. Luong, E.R. Smith, S.J. Smith, and M.W. Tubman, 2011. The Effects of DA-10 Removal on Circulation and Sediment Transport Potential within the Horn Island Pass and Lower Pascagoula Sound Channels. Final Report prepared for U. S. Army District, Mobile, AL.

Chapman R.S, E.J. Hayter, S.J. Smith, P.V. Luong, M. Tubman, A.S. Grzegorzewski, J.Z. Gailani, B.W. Bunch, D.H. Tillman. 2012. Hydrodynamic, Water Quality and Sediment Transport Modeling to Investigate the Impacts of Widening the Pascagoula Lower Sound and Bayou Casotte Navigation Channels. Final Report prepared for U. S. Army District, Mobile, AL.

Cheng, N.S. 1997. "Simplified settling velocity formula for sediment particles." *Journal of Hydraulic Engineering*, 123(2):149-152.

Chiriboga, E.D., and W.P. Mattes. 2008. "Buffalo Reef and substrate mapping project," Administrative Report 08-04. Great Lakes Indian Fish and Wildlife Indian Commission.

Demirbilek, Z., L. Lin, and A. Zundel. 2007. WABED model in the SMS: Part 2. Graphical interface. Coastal and Hydraulics Laboratory Engineering Technical Note ERDC/CHL CHETN-I-74. Vicksburg, MS: U.S. Army Engineer Research and Development Center.

Demirbilek, Z. and J.D. Rosati. 2011. Verification and validation of the Coastal Modeling System, Report 1: Summary Report, ERDC/CHL Technical Report 11-10, U.S. Army Corps of Engineers Research and Development Center, Vicksburg, MS.

Hayter, E.J., and S.J. Smith. 2010. "Numerical modeling studies supporting Port of Anchorage deepening and expansion - part iv; Numerical Sediment Transport Modeling." Proceedings 11th International Conference on Estuarine and Coastal Modeling; November 4-6, 2010, Seattle, WA 317-332.

Hayter E.J., R.S. Chapman, P.V. Luong, S.J. Smith, and D.B. Bryant. 2012. Demonstration of Predictive Capabilities for Fine-Scale Sedimentation Patterns within the Port of Anchorage, AK, Final Report prepared for U.S. Army District, Anchorage, AK.

James, S.C., C.A. Jones, M.D. Grace, and J.D. Roberts. 2010. "Advances in sediment transport modelling." *Journal of Hydraulic Research*, 48: 6, 754-763.

Jensen, R.E., Cialone, M.A., Chapman, R. S., Ebersole, B. E., Anderson, M. and L. Thomas, 2012. Modeling of Lake Michigan Storm Waves and Water Levels. Technical Report for the U.S. Army Engineer District, Detroit by the U.S. Army Engineer Research and Development Center, Vicksburg, MS.

Jones, C.A., and W. Lick. 2001. “SEDZLJ: A sediment transport model.” Final Report. University of California, Santa Barbara, California.

Lin, L., Z. Demirbilek, H. Mase, J. Zheng, and F. Yamada. 2008. “CMS-Wave: A Nearshore Spectral Wave Processes Model for Coastal Inlets and Navigation Projects.” U.S. Army Engineer Research and Development Center Technical Report ERDC-CHL TR-08-13. Vicksburg, MS.

Lin, L., Z. Demirbilek, and H. Mase. 2011a. Recent capabilities of CMS-Wave: A coastal wave model for inlets and navigation projects. Proceedings, Symposium to honor Dr. Nicholas Kraus. Journal of Coastal Research, Special Issue 59, 7-14.

Lin, L., Z. Demirbilek, R. Thomas, and J. Rosati. 2011b. Verification and validation of the Coastal Modeling System, Report 2: CMS-Wave, ERDC/CHL Technical Report 11-10, U.S. Army Corps of Engineers Research and Development Center, Vicksburg, MS.

Luong, P.V., and R.S. Chapman, 2009. “Application of Multi-block Grid and Parallelization Techniques in Hydrodynamic Modeling, DOD High Performance Computing Modernization Program: User Group Conference (HPCMP-UGC), San Diego, CA.

McNeil, J., C. Taylor, and W. Lick. 1996. “Measurements of the erosion of undisturbed bottom sediments with depth.” *Journal of Hydraulic Engineering*, 122(6):316-324.

Mehta, A.J. 2014. *An introduction to hydraulics of fine sediment transport*. Advanced series on Ocean Engineering: Volume 38. Hackensack, NJ: World Scientific.

Smith, J.M., D.T. Resio, and A. Zundel. 1999. STWAVE: Steady-state spectral wave model, Report 1: User’s manual for STWAVE Version 2.0. Coastal and Hydraulics Laboratory Instruction Report CHL-99-1. Vicksburg, MS: U.S. Army Engineer Waterways Experiment Station.

Snir, M., S. Otto, S. Huss-Lederman, D. Walker, and J. Dongarra. 1998. “MPI - The Complete Reference: Volume 1, the MPI Core”. MIT Press, Cambridge, MA.

STARR. 2012. “Great Lakes Storm Surge Analysis Lake Superior, FEMA Region V, Technical Support Data Notebook,” Contract No. HSFEHQ-09-D-0370, Task Order No. HSFE05-10-J-0007.

Sanford, L.P. 2008. "Modeling a dynamically varying mixed sediment bed with erosion, deposition, bioturbation, consolidation, and armoring." *Computers & Geosciences*, 34(10):1263-1283.

Smith, S.J., R.S. Chapman, D.J. Mark, and T.O. MacAlpin. 2008. "Hydrodynamic evaluation of proposed the Port of Anchorage expansion." Draft Report to POA, U.S. Army Engineer Waterways Experiment Station, Vicksburg, MS.

Smith, S.J., M.D. Peterson, and T.C. Pratt. 2010. "Numerical modeling studies supporting Port of Anchorage deepening and expansion; part ii: measuring physical processes." Proceedings 11th International Conference on Estuarine and Coastal Modeling, November 4-6, 2009, Seattle, WA. 286-300.

Snir, M., S. Otto, S. Huss-Lederman, D. Walker, and J. Dongarra. 1998. "MPI - The Complete Reference: Volume 1, the MPI Core." MIT Press, Cambridge, MA.

Van Rijn, L.C. 1984. "Sediment Transport: part i: bedload transport; part ii: suspended load transport: part iii: bed forms and alluvial roughness." *Journal of Hydraulic Engineering*, 110(10): 1431-1456; 110(11): 1613-1641, 110(12): 1733-1754.

Zundel, A. K. (2006). Surface-water modeling system reference manual – Version 9.2. Provo, UT: Brigham Young University Environmental Modeling Research Laboratory.

Appendix A

Description of SEDZLJ Sediment Transport Model

The sediment transport model in GSMB is the SEDZLJ sediment transport model (Jones and Lick 2001; James *et al*. 2010). SEDZLJ is dynamically linked to CH3D-MB in that the hydrodynamics and sediment transport modules are run during each model time step. A description of this sediment transport model is given next.

Suspended Load Transport of Sediment

The GSMB hydrodynamic module simulates the transport of each of the sediment classes to determine the suspension concentration for each size class in every water column layer in each grid cell. The transport of suspended sediment is determined through the solution of the following 3D advective-dispersive transport equation for each of the sediment size classes that is used in the model:

$$\frac{\partial C_i}{\partial t}+\frac{\partial uC_i}{\partial x}+\frac{\partial vC_i}{\partial y}+\frac{\partial (w-W_{Si})C_i}{\partial z}=\frac{\partial}{\partial x}\left(K_H\frac{\partial C_i}{\partial x}\right)+\frac{\partial}{\partial y}\left(K_H\frac{\partial C_i}{\partial y}\right)+\frac{\partial}{\partial \mathrm{z}}\left(K_v\frac{\partial C_i}{\partial z}\right)+S_i \quad \text{(A-1)}$$

where C_i = concentration of ith size class of suspended sediment, (u,v,w) = velocities in the (x,y,z) directions, t = time, W_{Si} = settling velocity of *ith* sediment size class, K_H = horizontal turbulent eddy diffusivity coefficient, K_V = vertical turbulent eddy diffusivity coefficient, and S_i = source/sink term for the *ith* sediment size class that accounts for erosion/deposition.

The settling velocities for noncohesive sediments are calculated in SEDZLJ using the following equation (Cheng 1997):

$$W_{\mathrm{s}}=\frac{\mu}{d}\left(\sqrt{25+1.2d_*^2}-5\right)^{\frac{3}{2}} \quad \text{(A-2)}$$

where μ = dynamic viscosity of water; d = sediment diameter; and d_* = non-dimensional particle diameter given by:

$$d_*=d\left[\left(\rho_{\mathrm{s}}/\rho_{\mathrm{w}}-1\right)g/\nu^2\right]^{1/3} \quad \text{(A-3)}$$

where ρ_w = water density, ρ_s = sediment particle density, g = acceleration due to gravity, and ν = kinematic fluid viscosity. Cheng's formula is based

on measured settling speeds of real sediments. As a result it produces slower settling speeds than those given by Stokes' Law because real sediments have irregular shapes and thus a greater hydrodynamic resistance than perfect spheres as assumed in Stokes' law.

The erosion and deposition of each of the sediment size classes, i.e., the source/sink term in the 3D transport equation given above, and the subsequent change in the composition and thickness of the sediment bed in each grid cell are calculated by SEDZLJ at each time step.

Description of SEDZLJ

SEDZLJ is an advanced sediment bed model that represents the dynamic processes of erosion, bedload transport, bed sorting, armoring, consolidation of fine-grain sediment dominated sediment beds, settling of flocculated cohesive sediment, settling of individual noncohesive sediment particles, and deposition. An active layer formulation is used to describe sediment bed interactions during simultaneous erosion and deposition. The active layer facilitates coarsening during the bed armoring process. The SEDZLJ model was designed to directly use the results obtained from a SEDFLUME study. A description of SEDFLUME is available at http://chl.erdc.usace.army.mil/CHL.aspx?p=s&a=ARTICLES;630. SEDFLUME is a straight, closed conduit rectangular cross-section flume in which detailed measurements of critical shear stress of erosion and erosion rate as a function of sediment depth are made using sediment cores (dominated by cohesive or mixed sediments) that are collected at the site to be modeled (McNeil *et al*. 1996). However, when SEDFLUME results are not available, it is possible to use a combination of literature values for these parameters as well as the results of SEDFLUME tests performed at other similar sites. In this case, a detailed sensitivity analysis should be performed to assist in quantifying the uncertainty that results from the use of these non-site specific erosion parameters.

Figure A-1 shows the simulated sediment transport processes in SEDZLJ. In this figure, U = near bed flow velocity, C = near bed sediment concentration, δ_{bl} = thickness of layer in which bedload transport occurs, U_{bl} = average bedload transport velocity, D_{bl} = sediment deposition rate for the sediment being transported as bedload, E_{bl} = sediment erosion rate for the sediment being transported as bedload, E_{sus} = sediment erosion rate for the sediment that is eroded and entrained into suspension, and D_{sus} =

sediment deposition rate for suspended sediment. Specific capabilities of SEDZLJ are listed below.

- Whereas a hydrodynamic model is calibrated to account for the total bed shear stress, which is the sum of the form drag due to bed forms and other large-scale physical features (*e.g.*, boulder size particles) and the skin friction (also called the surface friction), the correct component of the bed shear stress to use in predicting sediment resuspension and deposition is the skin friction. The skin friction is calculated in SEDZLJ as a function of the near-bed current velocity and the effective bed roughness. The latter is specified in SEDZLJ as a linear function of the mean particle diameter in the active layer.

- Multiple size classes of both fine-grain (*i.e.*, cohesive) and noncohesive sediments can be represented in the sediment bed. This capability is necessary in order to simulate coarsening and subsequent armoring of the surficial sediment bed surface during high flow events.

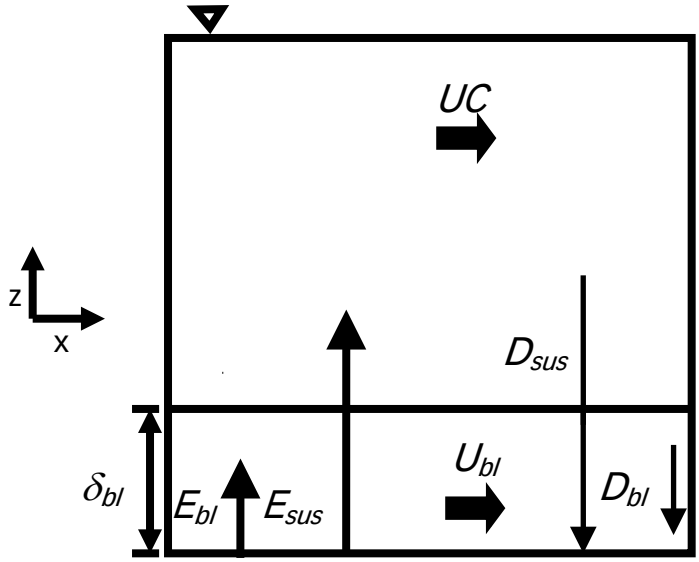

Figure A-1. Sediment transport processes simulated in SEDZLJ

- To correctly represent the processes of erosion and deposition, the sediment bed in SEDZLJ can be divided into multiple layers, some of which are used to represent the existing sediment bed and others that

are used to represent new bed layers that form due to deposition during model simulations. Figure A-2 shows a schematic diagram of this multiple bed layer structure. The graph on the right hand side of this figure shows the variation in the measured gross erosion rate (in units of cm/s) with depth into the sediment bed as a function of the applied skin friction. A SEDFLUME study is normally used to measure these erosion rates.

- Erosion from both cohesive and non-cohesive beds is affected by bed armoring, which is a process that limits the amount of bed erosion that occurs during a high-flow event. Bed armoring occurs in a bed that contains a range of particle sizes (*e.g.*, clay, silt, sand). During a high-flow event when erosion is occurring, finer particles (*i.e.*, clay and silt, and fine sand) tend to be eroded at a faster rate than coarser particles (i.e., medium to coarse sand). The differences in erosion rates of the various sediment particle sizes creates a thin layer at the surface of the sediment bed, referred to as the active layer, that is depleted of finer particles and enriched with coarser particles. This depletion-enrichment process can lead to bed armoring, where the active layer is primarily composed of coarse particles that have limited mobility. The multiple bed model in SEDZLJ accounts for the exchange of sediment through and the change in composition of this active layer. The thickness of the active layer is normally calculated as a time varying function of the mean sediment particle diameter in the active layer, the critical shear stress for resuspension corresponding to the mean particle diameter, and the bed shear stress. Figure A-3 shows a schematic of the active layer at the top of the multi-bed layer model used in SEDZLJ.

- SEDZLJ can simulate overburden-induced consolidation of cohesive sediments. An algorithm that simulates the process of primary consolidation, which is caused by the expulsion of pore water from the sediment, of a fine-grained, i.e., cohesive, dominated sediment bed is included in SEDZLJ. The consolidation algorithm in SEDZLJ accounts for the following changes in two important bed parameters: 1) increase in bed bulk density with time due to the expulsion of pore water, and 2) increase in the bed shear strength (also referred to as the critical shear stress for resuspension) with time. The latter parameter is the minimum value of the bed shear stress at which measurable

resuspension of cohesive sediment occurs. As such, the process of consolidation typically results in reduced erosion for a given excess bed shear stress (defined as the difference between the bed shear stress and bed shear strength) due to the increase in the bed shear strength. In addition, the increase in bulk density needs to be represented to accurately account for the mass of sediment (per unit bed area) that resuspends when the bed surface is subjected to a flow-induced excess bed shear stress. Models that represent primary consolidation range from empirical equations that approximate the increases in bed bulk density and critical shear stress for resuspension due to porewater expulsion (Sanford 2008) to finite difference models that solve the non-linear finite strain consolidation equation that governs primary consolidation in saturated porous media (Arega and Hayter 2008).

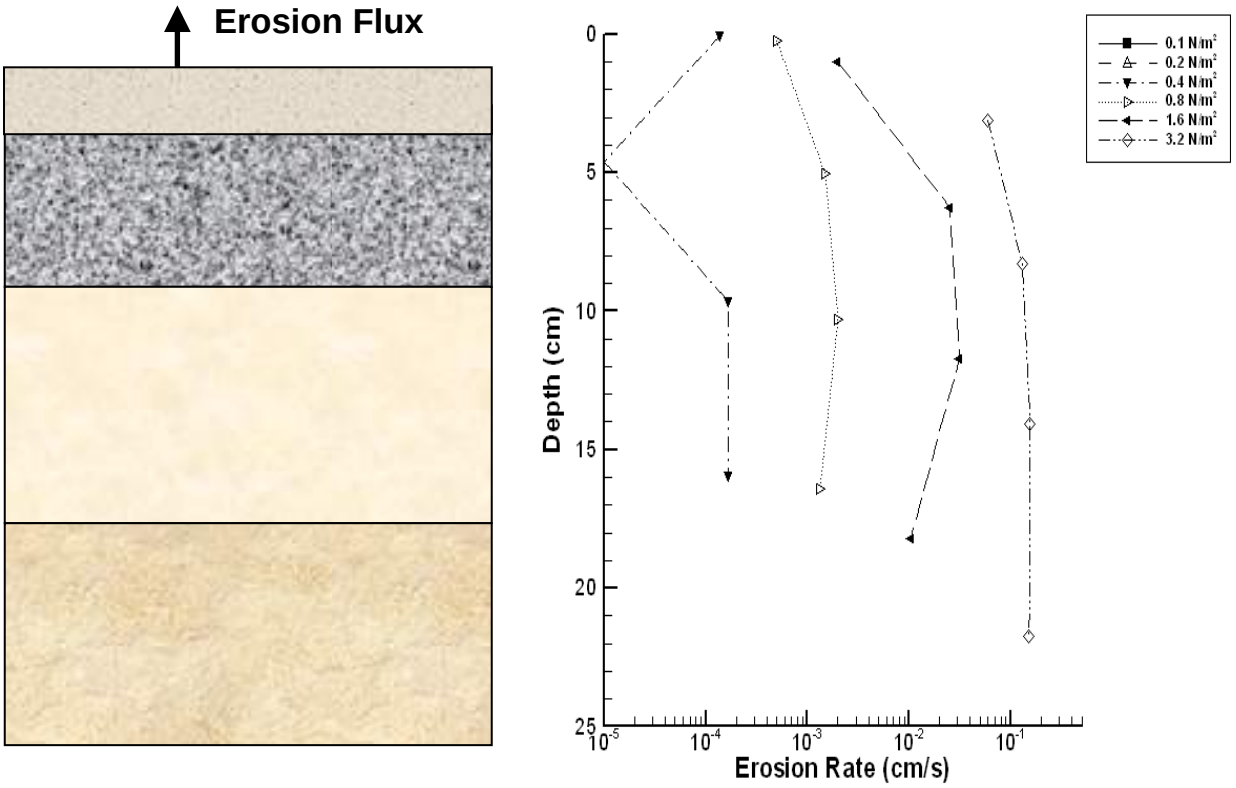

Figure A-2. Multi-Bed Layer Model used in SEDZLJ

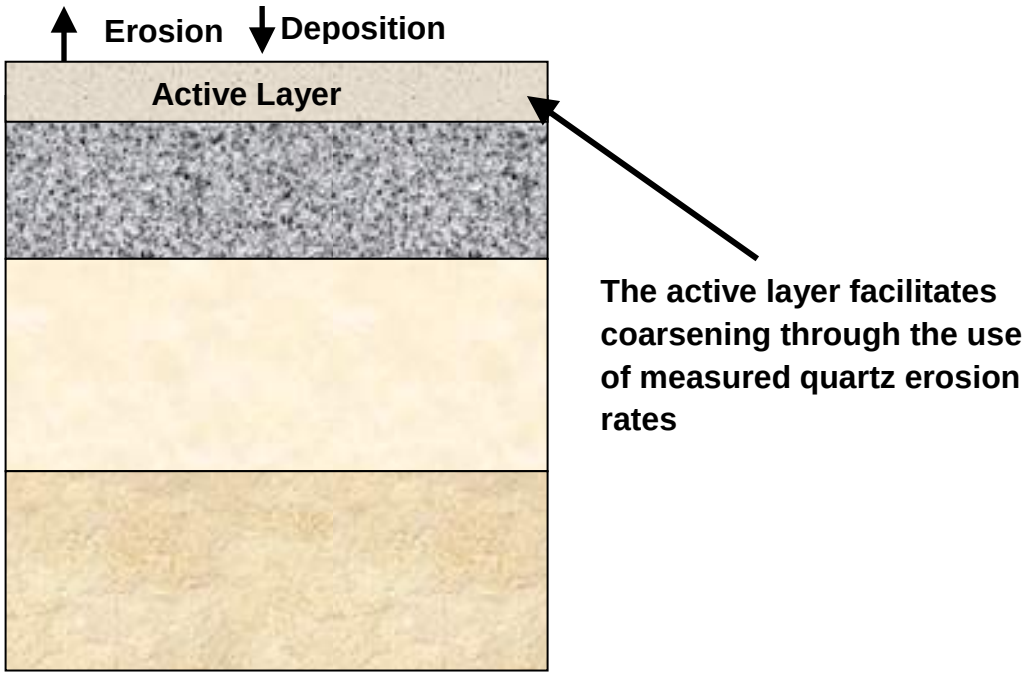

Figure A-3. Schematic of Active Layer used in SEDZLJ

An empirical-based consolidation algorithm is included in SEDZLJ. Simulation of consolidation requires performing specialized consolidation experiments to quantify the rate of consolidation. These experiments were not conducted as a component of this modeling study, and as such, consolidation was not simulated.

- SEDZLJ contains a morphologic algorithm that, when enabled by the model user, will adjust the bed elevation to account for erosion and deposition of sediment.

- SEDZLJ accounts for the effect of bed slope on erosion rates and bedload transport. The bed slopes in both the x- and y-directions are calculated, and scaling factors are applied to the bed shear stress, erosion rate, and bedload transport equations. A maximum adverse bed slope is specified that prevents bedload transport from occurring up too steep a slope.

Bedload Transport of Noncohesive Sediment

The approach used by Van Rijn (1984) to simulate bedload transport is used in SEDZLJ. The 2D mass balance equation for the concentration of sediment moving as bedload is given by:

$$\frac{\partial(\delta_{bl}C_b)}{\partial t} = \frac{\partial q_{b,x}}{\partial x} + \frac{\partial q_{b,y}}{\partial y} + Q_b \tag{A-4}$$

where δ_{bl} = bedload thickness; C_b = bedload concentration; $q_{b,x}$ and $q_{b,y}$ = x- and y-components of the bedload sediment flux, respectively; and Q_b = sediment flux from the bed. Van Rijn (1984) gives the following equation for the thickness of the layer in which bedload is occurring:

$$\delta_{bl} = 0.3 d d_*^{0.7} (\Delta\tau)^{0.5} \tag{A-5}$$

where $\Delta\tau = \tau_b - \tau_{ce}$; τ_b = bed shear stress, and τ_{ce} = critical shear stress for erosion.

The bedload fluxes in the x- and y-directions are given by:

$q_{b,x} = \delta_{bl} u_{b,x} C_b$

$q_{b,y} = \delta_{bl} u_{b,y} C_b$

where $u_{b,x}$ and $u_{b,y}$ = x- and y-components of the bedload velocity, u_b, which van Rijn (1984) gave as

$$u_b = 1.5\tau_*^{0.6}\left[\left(\frac{\rho_s}{\rho_w} - 1\right) g d\right]^{0.5} \tag{A-6}$$

with the dimensionless parameter τ_* given as

$$\tau_* = \frac{\tau_b - \tau_{ce}}{\tau_{ce}} \tag{A-7}$$

The x- and y-components of u_b are calculated as the vector projections of the CH3D Cartesian velocity components u and v.

The sediment flux from the bed due to bedload, Q_b, is equal to

$$Q_b = E_b - D_b \tag{A-8}$$

where E_b is the erosion of sediment into bedload, and D_b is the deposition of sediment from bedload onto the sediment bed.